

Invasive success of star weed (*Parthenium hysterophorus* L.) through alteration in structural and functional peculiarities

Ummar Iqbal¹, Zartasha Usman¹, Akkasha Azam¹, Hina Abbas¹, Khawaja Shafique K Ahmad^{Corresp.}²

¹ Botany, The Islamia University of Bahawalpur 64200, Rahim Yar Khan Campus, Rahim Yar Khan, Punjab, Pakistan

² Botany, University of Poonch Rawalakot, Rawalakot, Azad Kashmir, Pakistan

Corresponding Author: Khawaja Shafique K Ahmad
Email address: ahmadks@upr.edu.pk

A study was conducted on fifteen distinct populations of the star weed (*Parthenium hysterophorus* L.) to investigate the factors contributing to its widespread distribution in diverse environmental conditions. The results revealed significant variations in growth performance, physiological traits, and internal structures among populations from different habitats. The populations from wastelands exhibited superior growth, with higher accumulation of soluble proteins (TSP) and chlorophyll content (chl a, b, Tchl, car, and chl a/b). They displayed increased root and stem area, storage parenchyma, vascular bundle area, metaxylem area, and phloem area. Noteworthy leaf modifications included thicker leaves, sclerification around vascular bundles, and widened metaxylem vessels. Roadside populations possessed larger leaf area, enhanced antioxidant activity, increased thickness of leaves in terms of midrib and lamina, and a higher cortical proportion. Populations found in agricultural fields depicted enhanced shoot biomass production, higher levels of chlorophyll b, and an increased total chlorophyll/carotenoid ratio. Additionally, they exhibited increased phloem area in their roots, stems, and leaves, with a thick epidermis only in the stem. In conclusion, the study revealed explicit structural and functional variations among *P. hysterophorus* populations collected from different habitats. These variations were attributed to the environmental variability and could contribute to the widespread distribution of this species.

1 **Invasive success of star weed (*Parthenium hysterophorus* L.) through** 2 **alteration in structural and functional peculiarities**

3 Ummar Iqbal^{1*}, Zartasha Usman¹, Akkasha Azam¹, Hina Abbas¹, Khawaja Shafique Ahmad^{2*}

4 ¹Department of Botany, The Islamia University of Bahawalpur 64200, Rahim Yar Khan
5 Campus, Pakistan

6 ²Department of Botany, University of Poonch Rawalakot, Rawalakot 12350, AJK, Pakistan

7

8 *Corresponding author's e-mail: ahmadks@upr.edu.pk

9 **Abstract**

10 A study was conducted on fifteen distinct populations of the star weed (*Parthenium hysterophorus*
11 L.) to investigate the factors contributing to its widespread distribution in diverse environmental
12 conditions. The results revealed significant variations in growth performance, physiological traits,
13 and internal structures among populations from different habitats. The populations from
14 wastelands exhibited superior growth, with higher accumulation of soluble proteins (TSP) and
15 chlorophyll content (chl a, b, Tchl, car, and chl a/b). They displayed increased root and stem area,
16 storage parenchyma, vascular bundle area, metaxylem area, and phloem area. Noteworthy leaf
17 modifications included thicker leaves, sclerification around vascular bundles, and widened
18 metaxylem vessels. Roadside populations possessed larger leaf area, enhanced antioxidant
19 activity, increased thickness of leaves in terms of midrib and lamina, and a higher cortical
20 proportion. Populations found in agricultural fields depicted enhanced shoot biomass production,
21 higher levels of chlorophyll b, and an increased total chlorophyll/carotenoid ratio. Additionally,
22 they exhibited increased phloem area in their roots, stems, and leaves, with a thick epidermis only
23 in the stem. In conclusion, the study revealed explicit structural and functional variations among
24 *P. hysterophorus* populations collected from different habitats. These variations were attributed to
25 the environmental variability and could contribute to the widespread distribution of this species.

26 **Keyword:** *P. hysterophorus*, growth behavior, microstructural and functional modifications,
27 ubiquitous.

28

29 **Introduction**

30 Invasive species pose a significant threat to the diversity of native plant communities,
31 leading to the loss of ecological and economic values (McGeoch et al., 2010). One prominent
32 example of such an invasive species is *Parthenium hysterophorus* L., a perennial dicot herb
33 belonging to the Asteraceae family. This species is widely distributed and thrives in open and
34 disturbed environments. It is known to invade various habitats, including river banks, roadsides,
35 railway tracks, dry and moist areas such as mountainous regions, water channels, drains,
36 agricultural fields, open and barren lands, housing societies, and parking lots. Its ability to adapt
37 to different conditions has made it an ecological disaster, particularly in agricultural fields, where
38 it competes with crops for vital resources like water and minerals (Adkins and Shabbir, 2014).

39 Environmental stresses such as salinity and water deficit can have severe detrimental
40 effects on plant morphology and anatomy (Abideen et al., 2019; Zulfiqar et al., 2020). The
41 increasing scarcity of water in arid habitats is an alarming global issue that significantly limits
42 viable agriculture (Alvarez-Flores et al., 2018; Ali et al., 2020). Scientists are exploring various
43 techniques to promote resourceful and sustainable agricultural and horticultural practices (Zulfiqar
44 et al., 2019a). In response to water scarcity and other stresses, plants adopt various survival
45 strategies. They increase root biomass and reduce shoot growth, along with making changes in leaf
46 orientation, size reduction, and shedding (Leukovic et al., 2009; Oliveira et al., 2018). At the
47 anatomical level, these plants exhibit reduced cell size, enlargement in vascular tissues, alterations
48 in the xylem/phloem ratio, and reductions in xylem and phloem vessel size (Makbul et al., 2011;
49 Boughalleb et al., 2014). Additionally, under drought or salinity stress, plants significantly reduce
50 xylem vessel diameter and increase the thickness of epidermis, phloem, and mesophyll tissues in
51 aerial parts (El-Afry et al., 2012). They also accumulate substantial amounts of protective
52 compounds like glycine betaine, proline, and total soluble proteins to combat the adverse effects
53 of these abiotic stresses. Ionic homeostasis is a crucial physiological mechanism in plants that
54 contributes to their vitality and vigor even under harsh conditions (Siringam et al., 2011). This
55 mechanism involves processes such as noxious ion accumulation, selective ion uptake, and
56 excretion of toxic ions through specialized structures like leaf hairs, trichomes, leaf sheaths, and
57 excretory organs (Hameed et al., 2009).

58 *Parthenium hysterophorus* L. is a widely spread and aggressive annual herbaceous weed. This
59 weed is known for its robust growth and high reproductive capacity, particularly in warm climates.

60 It is native to northeast Mexico and endemic to America (Adkins and Shabbir, 2014). Over the
61 past century, it has spread to Africa, Australia, Asia, and Pacific Islands, becoming one of the most
62 destructive and hazardous weeds worldwide. It is commonly found in abandoned lands, residential
63 areas near towns, along roadsides, railway tracks, dry mountains, scrub forests, and drainage and
64 irrigation canals. It is often grown as an ornamental plant in gardens, plantations, and cultivated
65 crops. The weed's high reproductive capacity allows a single plant to produce between 10,000 to
66 15,000 viable seeds, which can disperse and germinate, rapidly covering large areas (Maharjan et
67 al., 2020).

68 To investigate the hypothesis regarding *P. hysterophorus* response to environmental stresses, a
69 study was conducted to explore various aspects. The study aimed to answer the following
70 questions: a) how does *P. hysterophorus* respond to heterogeneous environmental conditions at
71 the levels of growth, anatomy, and physiology? b) What types of micro-structural, physiological,
72 and morphological adaptations enable *P. hysterophorus* to mitigate the detrimental effects of
73 abiotic stresses? c) Are the induced micro-structural and physiological modifications specific to
74 certain environmental conditions? d) Can the resistance mechanisms and alterations be classified
75 based on the population's behavior in relation to their respective environments? e) Do all
76 populations of *P. hysterophorus* exhibit both internal and external responses to the prevailing
77 climatic conditions? The study aimed to shed light on the mechanisms and adaptations employed
78 by *P. hysterophorus* to cope with environmental stresses. By examining the responses and
79 modifications at different levels, the researchers sought to gain a comprehensive understanding of
80 the weed's ability to thrive in diverse environmental conditions.

81 **Materials and Methods**

82 **Study surveys, sampling and collection sites**

83 *Parthenium hysterophorus* populations were sampled from ecologically distinct regions of Punjab
84 province to determine the growth, physiological and anatomical response towards heterogenic
85 environmental conditions (Fig. 1 & 2, Table 1). The sampling was done during the peak of
86 flowering season (March to April) in year 2021. Each study site was thoroughly search in radius
87 of 1km and total 50 plants were ear marked. Ten plants (n=10) per population were finalized for
88 the measurement of morpho-anatomical and physiological parameters. The populations were
89 collected from five prominent ecological regions such as i) near wasteland (RYK-Rahim Yar

90 Khan, SDK-Sadiqabad, KHP-khanpur), ii) along water channels (BWP-Bahawalpur, LAP-
91 Liaquatpur, AHP-Ahmadpur, MUL-Multan), iii) along roadside (VEH-Vehari, DGK-DG Khan,
92 RJP-Rajanpur, JHG-Jhang), iv) near agriculture fields (MUZ-Muzaffargarh, SAR-Sargodha, FSD-
93 Faisalabad, LYH-Layyah). Coordinates were measured with the help of google positioning system
94 (GPS, model: Garmin E-Trex 20, GPS accuracy ± 1 m) (Table 2). Climatic data was taken from
95 meteorological department situated in each district.

96 **Soil physiological parameters**

97 The soil texture was assessed using the USDA textural triangle, which categorizes soils into
98 distinct textural classes according to the relative proportions of sand, silt, and clay present in the
99 soil sample. The Walkley method (1947) was employed to measure the organic matter content in
100 the soil. This method involves oxidation of organic matter by dichromate in the presence of sulfuric
101 acid. A combined pH and EC meter (WTW series InoLab pH/Cond 720, USA) was used to
102 measure the soil pH and ECe. Saturation paste, prepared by saturating the soil with water and
103 extracting the solution, was used for these measurements. The saturation paste was analyzed to
104 determine the concentrations of different ions, including Na^+ , K^+ , and Ca^{2+} , utilizing a flame
105 photometer (Jenway, PFP-7, UK). The nitrogen content in the soil was assessed using the micro-
106 Kjeldahl method, which involves digesting the soil sample with sulfuric acid. The resulting
107 ammonia was then distilled and titrated using a semi-automatic ammonia distillation unit (UDK-
108 132, NIB-B (3)-DSU-003 Italy). The soil phosphorus content was measured following the protocol
109 described by Wolf in 1982. This method typically involves extracting the available phosphorus
110 from the soil using a suitable extractant, followed by colorimetric analysis. The chloride content
111 in the soil was assessed using the Mohrs' titration method. This method, developed by Mohrs in
112 1856, involves titrating a solution containing the extracted chloride ions with a silver nitrate
113 solution to determine the chloride concentration. To determine the soil saturation percentage, the
114 soil samples were dried in an oven at 70°C , and 200 g of the dried soil was used to prepare a
115 composite saturation paste, which was then analyzed. Saturation percentage assayed by following
116 formula:

$$117 \quad SP (\%) = \frac{\text{Amount of water added}(g)}{\text{Oven dried soil}(g)} \times 100$$

118 Where SP % is saturation percentage.

119

120 **Morphological parameters**

121 To collect the necessary measurements, a meter rod was utilized to directly measure the height of
122 the plant, as well as the lengths of both the shoot and root. A digital loading balance was employed
123 to determine the fresh weights of the shoot and root. Immediately after harvesting, the plant parts
124 were weighed to obtain their fresh weights. For dry weight analysis, the plant samples were
125 subjected to oven-drying at a temperature of 65 °C until a constant weight was achieved. This
126 ensured the complete removal of moisture from the samples. The dry weights of the shoot and root
127 were then measured using a digital loading balance. To assess the leaf characteristics, the number
128 of leaves on each plant was manually counted. The leaf area was determined using cm-graph paper,
129 providing a quantitative measurement of the area occupied by the leaves. The leaf area was
130 calculated using a formula provided by Lopes et al. (2016).

131 **Physiological parameters**

132 *Osmolytes and soluble proteins*

133 Fresh samples were taken in falcon tubes and stored (-80 °C) for chlorophyll pigments,
134 osmoprotectants, and antioxidants activity. For the analysis of proline, fresh leaf samples were
135 thoroughly homogenized in sulfo-salicylic acid. Then was transferred into cuvette containing
136 ninhydrin solution. After subjected to water bath (100 °C) toluene was added for extraction of
137 proline. Lastly, readings were taken on a spectrophotometer (Model 220, Hitachi, Japan) at 520
138 nm wavelength (Bates et al., 1973).

$$139 \quad \text{Proline } (\mu\text{mol g}^{-1} \text{ fresh weight}) = \frac{\mu\text{g proline ml}^{-1} \times \text{ml of toluene}/115.5}{\text{sample weight (g)}}$$

140

141 To measure the glycine betaine content in the leaf samples, fresh leaf samples weighing 0.5 g were
142 soaked in 20 ml of deionized water (H₂O) at a temperature of 25 °C for a duration of 24 hours.
143 Following the soaking period, an extract was prepared from the soaked samples and assayed using
144 the established protocols outlined by Grattan and Grieve (1998). For the analysis of total soluble
145 proteins, fresh leaf samples weighing 0.2 g were sliced and thoroughly crushed in 5 ml of
146 phosphate buffer at a pH of 7.0. The buffer facilitated the extraction of proteins from the crushed
147 leaf samples. The mixture of crushed leaf samples and buffer was then subjected to centrifugation
148 at 5000 rpm for 5 minutes. This centrifugation step effectively separated the solid components of
149 the mixture from the liquid supernatant. The supernatant, containing the soluble proteins, was

150 collected for further analysis. To quantify the protein content in the supernatant, the method
 151 developed by Lowry et al. (1951) was employed. This method relies on a colorimetric assay to
 152 measure the protein concentration present in the sample

153 *Photosynthetic parameters*

154 To estimate the photosynthetic pigments, including chlorophylls (chl_a, chl_b, and total chl.) and
 155 carotenoids, the methods described by Arnon in 1949 and Davis in 1979 were followed. A
 156 spectrophotometer (Hitachi-220, Japan) was used for the measurements. The formulas used for
 157 calculations were:

$$159 \quad \text{Chl. a (mg g}^{-1} \text{ f.wt.)} = [12.7(\text{OD663}) - 2.69(\text{OD645})] \times \frac{V}{1000} \times W$$

$$160 \quad \text{Chl. b (mg g}^{-1} \text{ f.wt.)} = [22.9(\text{OD645}) - 4.68(\text{OD663})] \times \frac{V}{1000} \times W$$

$$161 \quad \text{Total chl. (mg g}^{-1} \text{ f.wt.)} = [20.2(\text{OD645}) - 8.02 (\text{OD663})] \times \frac{V}{1000} \times W$$

$$162 \quad \text{Carotenoids (mg g}^{-1} \text{ f.wt.)} = [12.7(\text{OD480}) - 0.114 (\text{OD663})] - 0.638 (\text{OD645}) / 2500$$

163 *Total antioxidant activity*

164 For the measurement of total antioxidant activity, a dried leaf sample weighing 0.5 g was placed
 165 in a test tube. To facilitate the extraction of antioxidants from the leaf tissue, 20 mL of a 0.45%
 166 salt solution was added to the test tube. The sample was then subjected to heating in a water bath
 167 at 40°C for a duration of 20 minutes. After the heating process, the test tube was centrifuged at
 168 3000 rpm for 30 minutes, enabling the separation of the supernatant from the solid residue. The
 169 supernatant, which contained the extracted antioxidants, was carefully separated and stored at -
 170 20°C until further analysis. To measure the total antioxidant activity, the FTC (Ferric Thiocyanate)
 171 method described by Rahmat et al. (2003) was employed. This method involves assessing the
 172 ability of the antioxidants to inhibit lipid peroxidation by reacting with ferric ions.

173 **Anatomical parameters**

174 To examine the anatomy of the root, stem, and leaf, the largest ramet from each replicate was
 175 selected. For leaf anatomy, a 2 cm section was obtained from the leaf base of fully mature and sun-
 176 exposed leaves. For stem anatomy, a section was taken from the base of the internode of the main
 177 tiller. Similarly, for root anatomy, a section was obtained from the thickest adventitious root near
 178 the junction of the root and shoot. The collected plant material was fixed using a formaldehyde

179 acetic alcohol solution consisting of 10% formaldehyde, 5% acetic acid, 50% ethanol, and 35%
180 distilled water. The plant material was immersed in the fixative solution for 48 hours, followed by
181 transfer to an acetic alcohol solution containing 25% acetic acid and 75% ethanol for long-term
182 storage. To prepare the sections for microscopic analysis, free-hand sections were made from the
183 fixed plant material. These sections underwent a series of dehydration steps using ethanol. For
184 staining, the sections were subjected to the standard safranin and fast green double-staining
185 technique, as outlined by Ruzin (1999). Measurements of the sections were taken using a light
186 microscope (Nikon SE Anti-Mould, Japan) equipped with an ocular micrometer that was calibrated
187 using a stage micrometer. Micrographs of the stained sections were captured using a digital camera
188 (Nikon FDX-35) mounted on a stereomicroscope (Nikon 104, Japan).

189 **Statistical analysis**

190 The morphological, physiological, and anatomical trait data were subjected to statistical analysis
191 using a One-way analysis of variance (ANOVA) in a complete randomized design with ten
192 replicates. Mean values were compared using the least significant difference (LSD) test at a
193 significance level of 5%. The statistical analysis was conducted using the Minitab software
194 package (version 17.1.0, Pennsylvania State University, USA). To examine the relationships
195 between the different morphological, physiological, and anatomical traits and the soil
196 physicochemical parameters of the collection sites, Principal Component Analysis (PCA) was
197 conducted. The analysis was carried out using the R-studio software, and the data were plotted to
198 visualize the patterns and associations. Furthermore, heatmaps were constructed using the
199 pheatmap package in R-studio. These heatmaps were used to cluster the selected groups based on
200 (i) soil physicochemical attributes and morphophysiological parameters, (ii) soil physicochemical
201 attributes and root anatomy, (iii) soil physicochemical attributes and stem anatomy, and (iv) soil
202 physicochemical attributes and leaf anatomy. The heatmaps provide a visual representation of the
203 relationships and similarities among the different variables.

204 **Results**

205 *Soil physicochemical characteristics*

206 The soil in most of the habitats was sandy (Table 2). The loamy soil was observed in four habitats
207 RYK (near the wasteland), KHP (near waste deposit), VEH (near the roadside), FSD (along rice
208 field) and LYH (wheat field) whereas loamy sand was observed in two habitats such as MLN

209 (along river Chenab) and SAR (along sorghum field). Clayey loam was seen in MUZ habitat (near
210 cotton field). The soil electrical conductivity of soil ranged from 0.76 to 6.73 dSm⁻¹, the maximum
211 value of soil ECe was recorded at RYK (near the wasteland) and KHP (near waste deposit) sites
212 and the minimum was observed at SDA (along barren land) and RJP (near M5 motorway). Habitats
213 like water channel (LAP), along road side (VEH) and near agriculture field (FSD) showed
214 exceptionally highly level of soil ECe than rest of the populations. Most of the habitat comprised
215 of alkaline pH, ranging from 7.8 to 8.9. The acidic pH was observed only in one habitat RYK (near
216 the wasteland). The soil organic matter was varied from 0.21 to 0.56%. the maximum OM was
217 noted in soil of Chenab river (MLN) and the minimum was measured in soil of roadside population
218 (VEH). The soil saturation percentage ranged from 15 to 42%. The maximum SP was observed
219 in soil of wheat filed (FSD) population. It was the minimum in soil of water canal (LAP) and rice
220 filed (FSD) populations. The soil Phosphate concentration varied from 1.6 mg L⁻¹ in the LAP and
221 FSD habitats to 3.6 mg L⁻¹ in the LYH habitat. The nitrate content in the LYH habitat exhibited
222 the highest value, while the DGK habitat recorded the lowest value. The soil chloride ion (Cl⁻)
223 content reached its maximum (567.8 mg L⁻¹) in the RYK habitat, while the minimum (72.1 mg
224 L⁻¹) was observed in both the MLN and MUZ habitats. The soil's calcium ion (Ca²⁺) concentration
225 ranged from 54.2 to 156.1 mg L⁻¹. The RYK habitat showed the highest soil calcium concentration,
226 while the SDA habitat exhibited the lowest. The soil sodium ion (Na⁺) content ranged between
227 54.2 and 398.9 mg L⁻¹, with the RYK population having the highest value and the SDA habitat
228 recording the lowest. The maximum soil potassium ion (K⁺) concentration was observed in the
229 MLN and LYH habitats, while the minimum was found in the SDA habitat.

230 ***Growth characteristics***

231 Plant height was the maximum (56.5cm) in BWP population and the minimum (16.3 cm)
232 in FSD population (Fig. 2, Table 3). The maximum shoot length (44.7 cm) was recorded in BWP
233 population while the minimum (11.3 cm) of this parameter was noted in FSD population. Three
234 populations, KHP, VEH and SAR showed maximum shoot fresh (11.5 g plant⁻¹) and dry weight
235 (5.8 g plant⁻¹), while population FSD had least shoot fresh (3.0 g plant⁻¹) and dry weight (1.2 g
236 plant⁻¹). Root length was the maximum (11.5 cm) in BWP and the minimum (4.5 cm) in VEH
237 population. Four populations namely RYK, KHP, LAP and SAR showed maximum root fresh
238 weight (1.5 g plant⁻¹), while the population RJP exhibited low value of dry weight (0.4 g plant⁻¹).
239 Population RYK showed the maximum dry weight (1.2 g plant⁻¹) and populations BWP, AHP,

240 RJP and LYH possessed the minimum dry weight (0.2 g plant^{-1}). The maximum number of leaves
241 (29.5) were recorded in RYK population, while their minimum value (9.0) was observed in FSD
242 population. Two populations, BWP (65.3 cm^2) and VEH (65.4 cm^2) showed the maximum value
243 of leaf area, while the minimum (14.9 cm^2) of that parameter was measured in RYK population.

244 *Physiological characteristics*

245 The population from RYK exhibited the highest total soluble protein content ($47.9 \mu\text{g g}^{-1} \text{ d.wt.}$),
246 while the population from VEH had the lowest ($9.4 \mu\text{g g}^{-1} \text{ d.wt.}$) (Table 3). Population BWP
247 showed the maximum proline content ($19.8 \mu\text{mol g}^{-1} \text{ d.wt.}$), whereas populations AHP and LYH
248 possessed the minimum ($1.6 \mu\text{mol g}^{-1} \text{ d.wt.}$). Glycine betaine content was highest in the BWP
249 population ($10.2 \mu\text{mol g}^{-1} \text{ d.wt.}$) and lowest in the FSD population ($1.3 \mu\text{mol g}^{-1} \text{ d.wt.}$). For
250 chlorophyll a content, the SDA population had the highest value ($2.4 \text{ mg g}^{-1} \text{ f. wt.}$), while
251 populations MUL, DGK, RJP, JHG, and FSD had the lowest value ($1.3 \text{ mg g}^{-1} \text{ f. wt.}$). Four
252 populations, SDA, JHG, MUZ, and FSD, showed the highest chlorophyll b content ($2.0 \text{ mg g}^{-1} \text{ f.}$
253 wt.), whereas the RYK population showed the lowest value ($0.3 \text{ mg g}^{-1} \text{ f. wt.}$). The SDA
254 population had the maximum total chlorophyll content ($4.4 \text{ mg g}^{-1} \text{ f. wt.}$), while the RYK and
255 DGK populations had the minimum ($2.1 \text{ mg g}^{-1} \text{ f. wt.}$). The LAP population had the highest
256 carotenoid content ($2.8 \text{ mg g}^{-1} \text{ f. wt.}$), and the MUZ population had the lowest ($1.0 \text{ mg g}^{-1} \text{ f. wt.}$).
257 The chlorophyll a/b ratio was highest in the RYK population (6.3) and lowest in the SAR
258 population (0.3). The MUZ population had the maximum total chlorophyll/carotenoid ratio (3.7),
259 whereas the VEH population had the minimum (0.3). Antioxidant activity was the maximum (9.9
260 %) in three populations, MUL, VEH and DGK, whereas it was the minimum (3.5%) in LAP
261 population.

262 *Anatomical characteristics*

263 Root anatomy

264 The maximum root area ($400.4 \mu\text{m}^2$) was recorded in two populations, SAR and RYK, whereas
265 the minimum ($259.1 \mu\text{m}^2$) was in FSD population (Fig. 3, Table 4). The population from MUL
266 had the maximum epidermal thickness ($31.4 \mu\text{m}$), while the population from LYH had the
267 minimum epidermal thickness ($9.4 \mu\text{m}$). Population RYK showed the maximum cortical thickness
268 ($94.2 \mu\text{m}$), and population FSD did the smallest ($31.4 \mu\text{m}$). The maximum value of cortical cells
269 ($41.1 \mu\text{m}$) were recorded in RYK and KHP populations, whereas their minimum value ($7.4 \mu\text{m}^2$)
270 was seen in two populations, MUZ and SAR. Population BWP possessed the largest vascular

271 bundles ($121.3 \mu\text{m}^2$) than rest of the populations. On the other hand, population MUL had smallest
272 vascular bundles ($55.0 \mu\text{m}^2$). Three populations namely KHP, BWP and MUZ exhibited widened
273 metaxylem vessels ($15.7 \mu\text{m}^2$), whereas the populations of VEH and SAR had the narrowest
274 vessels ($9.4 \mu\text{m}^2$). Phloem area was the maximum ($2.5 \mu\text{m}^2$) in four populations, KHP, LAP, MUZ
275 and FSD, but the minimum ($0.5 \mu\text{m}^2$) was recorded in BWP and JHG.

276 Stem anatomy

277 The maximum value of stem area ($440.4 \mu\text{m}^2$) was observed in populations KHP and MUZ, while
278 their minimum value ($182.6 \mu\text{m}^2$) was noted in JHG (Fig. 4, Table 4). Epidermal thickness was
279 the maximum ($23.6 \mu\text{m}$) in SAR and KHP, and the minimum ($9.4 \mu\text{m}$) in RYK and RJP.
280 Population KHP showed the highest cortical proportion ($70.7 \mu\text{m}$), whereas the populations of
281 RYK and MUL had lowest region ($18.8 \mu\text{m}$) of that character. Cortical cells area was the maximum
282 ($14.1 \mu\text{m}^2$) in population AHP, FSD and LYH, and the minimum ($6.3 \mu\text{m}^2$) was in BWP.
283 Population AHP and KHP showed largest vascular bundles ($164.9 \mu\text{m}^2$) as compared to other
284 populations, while populations of RYK, SDA and FSD represented smallest vascular regions (94.2
285 μm^2). The maximum value of metaxylem vessels ($18.8 \mu\text{m}^2$) were recorded in KHP and MUL, and
286 their minimum value ($9.4 \mu\text{m}^2$) was noted in BWP, VEH, MUZ and LYH populations. Phloem
287 area was the maximum ($69.1 \mu\text{m}^2$) in population LYH, and the minimum ($14.1 \mu\text{m}^2$) in SDA.

288 Leaf anatomy

289 Leaf thickness greatly varied in all populations of *P. hysterophorus* (Fig. 5, Table 4). Midrib
290 thickness was the maximum ($420.8 \mu\text{m}$) in SDA, and the minimum ($235.5 \mu\text{m}$) in FSD population.
291 The maximum value of lamina thickness ($38.1 \mu\text{m}$) was observed in population VEH, while the
292 minimum value ($11.0 \mu\text{m}$) was observed in RJP. Thicker epidermis ($23.6 \mu\text{m}$) was measured in
293 three populations, KHP, LAP and AHP, whereas the thinner ($10.6 \mu\text{m}$) of this parameter was noted
294 in MUL. Enhanced cortical region ($185.3 \mu\text{m}$) was observed in VEH, and their reduced (100.1
295 μm) was in FSD. The population from roadside habitats (VEH) exhibited the largest cortical cells,
296 while the populations from FSD and LYH had the smallest cortical cells. The vascular bundle area
297 was highest in the SDA population, whereas the RYK population had the lowest vascular bundle
298 area. Among the populations, SDA had the highest number of metaxylem vessels, while BWP had
299 the fewest. The phloem area was greatest in the SAR population, but was minimal in the KHP and
300 AHP populations.

301 **Multivariate analysis**

302 **Principal component analysis (PCA)**

303 Principal component analysis (PCA1) exhibited 27.4% and 21.2% (48.6%) variability among
304 morpho-physiological and soil physicochemical characteristics of *P. hysterophorus*. The Chl a,
305 TChl/Car, TChl, RDW, RFW, SFW and GB showed strong influence of soil NO₃, SP, PO₄ and
306 pH, whereas Chl b, Chl a/b, TSP, SDW, SL, RL and LA represented least influence of soil OM
307 (Fig. 6A). Principal component analysis revealed significant influence of soil physiochemical
308 characters on anatomical traits of species. PCA2 represented the variability of 33.2% and 18.4%
309 (51.6%) among root anatomy and soil physicochemical attributes, as the CCA showed close
310 influence of soil Ca, ECe, Cl and Na, while MA, RA, CT, EpT, PhA and VBA had least influence
311 of soil OM (Fig. 6B). PCA3 indicated 36.5% and 18.9% (55.4%) variations between stem anatomy
312 and soil parameters, for example the MA represented very close influence of soil K and NO₃,
313 whereas the CCA showed with soil ECe and VBA with soil pH (Fig.6C). PCA4 exhibited 28.8%
314 and 19.9% (58.8%) variability amid leaf anatomy and soil attributes, as the LMT, Mrt and CCA
315 showed strong influence of soil N₀₃, K, SP and PO₄, while the EPT with soil Ca and Cl, and the
316 VBA and PhA with soil pH (Fig. 6D).

317 **Clustered heatmaps**

318 Heatmap between soil physicochemical characters and morpho-physiological attributes exhibited
319 six major clusters (Fig. 7A). In first cluster, soil attribute, OM form cluster with Ca and Car
320 content. The second cluster indicated the clustering of soil ECe, Cl and Na with LN, RFW and
321 RDW. In third cluster, RL form cluster with chlb, Tchl, TSP and GB. The fourth group showed
322 clustering of soil attributes K, NO₃, SP and PO₄. The fifth cluster exhibited the clustering of LA
323 and soil pH, and the sixth cluster showed the clustering of Chl a/b, Chla and TChl/Car. The seventh
324 cluster indicated the clustering of SDW, SFW, PH and SL. Heatmap between root anatomical
325 characteristics and soil attributes indicated four major clusters (Fig. 7B). The first cluster indicating
326 the clustering of OM and MA. In the second cluster, soil pH form cluster with RA, CT, PhA, EpT
327 and VBA. In the third cluster, soil attributes like NO₃, K, SP and PO₄ form clustering. In the
328 fourth cluster, soil Ca, Na, ECe and Cl showed clustering with CCA.

329 Heatmap between soil physicochemical attributes and stem anatomical features exhibited three
330 clusters (Fig. 7C). In the first cluster, soil pH and OM form clustering with VBA, EpT and PhA.
331 In the second cluster, soil ECe, Cl, Na and Ca showing clustering with CCA and CT. The third
332 cluster indicated the clustering of K, PO₄, SP and NO₃ with MA. Heatmap between soil

333 physicochemical attributes and leaf anatomical features exhibited four clusters (Fig. 7D). In the
334 first cluster, soil OM and pH form cluster with PhA and VBA, whereas in the second cluster, soil
335 NO₃, SP and PO₄ form cluster with LMT and CCA. The third cluster indicating the clustering of
336 EPT and CT, while the fourth cluster showing clustering of soil ECe, NA, Cl and Ca with MrT
337 and MA.

338 **Discussion**

339 The evaluation of morpho-anatomical and physio-biochemical adaptive markers is crucial for
340 understanding the underlying mechanisms of adaptation in differently adapted populations to
341 multiple stresses (Hameed et al., 2011). In the face of severe drought conditions or physiological
342 drought induced by other environmental stresses, water conservation becomes a primary strategy
343 (Sun et al., 2018). In water-scarce conditions, water conservation in plants is achieved through
344 mechanisms such as water storage in parenchymatous tissues like pith and cortex (Alvarez et al.,
345 2008), efficient water translocation facilitated by widening of vessels, and reduction of water loss
346 through the presence of mechanical tissues and a thick cuticle on the surface of plant organs (Micco
347 and Aronne, 2012). To evaluate the strength of adaptation and the extent of these adaptations in
348 plant survival, populations of *P. hysterophorus* were sampled from a wide range of habitats.

349 The investigation revealed significant variations in morphological characteristics among the
350 populations of *P. hysterophorus*, which can be attributed to the diverse environmental conditions
351 in which these populations were originally adapted. Under the controlled conditions of the study,
352 the genetically fixed characteristics of each population were expressed, reflecting their adaptation
353 to their respective habitats (Mojica et al., 2012; Paccard et al., 2013). The population from the
354 BWP site, which is located along a water channel with relatively soft soil texture, exhibited the
355 maximum growth (as shown in Table 3). This type of habitat seems to be more favorable for the
356 growth and development of *P. hysterophorus*, as reported for other hydrophytes (Qadir et al., 2008;
357 Hasanuzzaman et al., 2014). The compactness of the soil directly influenced the growth and
358 propagation of the species, with habitats consisting of compact soil showing shorter plants, such
359 as the FSD and VEH populations. Similar findings were reported by Hamza and Anderson (2005),
360 who observed shorter stature plants in compact soil. Biomass production, both in roots and shoots,
361 is a reliable criterion for assessing tolerance potential of a species (Khosroshahi et al., 2014). The
362 RYK and KHP populations demonstrated good overall growth response, indicating their potential
363 for stress tolerance. The SAR population also exhibited vigorous growth, suggesting its complete

364 adaptation to its specific habitat. Root and shoot parameters, such as length, number, fresh and dry
365 weights, have been previously associated with abiotic stresses like drought or physiological
366 drought in other plant species (Talukdar, 2013; Ye et al., 2015). The RYK population displayed a
367 high number of leaves per plant, although they were smaller in size. Having a large number of
368 leaves can enhance a plant's photosynthetic efficiency (Weraduwege et al., 2015), while smaller
369 leaves can increase water use efficiency by reducing transpiration rates (Medrano et al., 2015).
370 This adaptation is particularly important for survival in harsh saline desert conditions.

371 Chlorophyll pigments serve as sensitive indicators of the metabolic state under salt stress
372 conditions (Chattopadhyay et al., 2011). In the present study, the least saline population SDA and
373 moderately saline population KHP showed an increase in chlorophyll a, chlorophyll b, total
374 chlorophyll, and carotenoid content. Similar findings have been reported by Amirjani (2011) and
375 Sarabi et al. (2017). Conversely, the highly saline population RYK exhibited lower amounts of
376 chlorophyll pigments and carotenoids. This decrease in pigment content aligns with other studies
377 that have reported a significant reduction in photosynthetic pigments under highly saline
378 conditions, such as López-Millán et al. (2009) in *Lycopersicon esculentum*, Peng et al. (2013) in
379 *Elsholtzia splendens*, and Sytar et al. (2013) in various plant species. In the present study, the BWP
380 population showed an increasing trend in organic osmolytes. The accumulation of osmolytes is an
381 effective strategy employed by plants to endure prevailing, which serves as a defensive mechanism
382 for plants to maintain turgor pressure and prevent tissue collapse due to desiccation (Kholodova et
383 al., 2010; Sun et al., 2010). Elevated levels of total antioxidant activity were observed in *P.*
384 *hysterophorus* populations inhabiting roadside areas, such as VEH and DGK. These findings align
385 with previous studies conducted by Nadgorska-Socha et al. (2013), Zemanova et al. (2013), and
386 Almohisen (2014), which demonstrated that dust pollution stimulates the production of various
387 metabolites in plants. These metabolites play a crucial role in mitigating stress by activating the
388 plants' defense systems (Sharma & Dietz, 2006).

389 The anatomical characteristics of plants have been recognized as highly responsive to climatic
390 conditions (Caemmerer and Evans, 2015). This adaptability enables plants to thrive and survive in
391 challenging environment (De Micco and Aronne, 2012). The size of the root cross-sectional area
392 is predominantly determined by the relative proportions of the cortical region and the vascular
393 bundle area, as indicated in Table 4. An expansion in root area not only enhances the capacity for
394 water storage but also strengthens the mechanical integrity of the plant's soft tissues, enabling

395 efficient transport of water and minerals. The observed increase in root cross-sectional area
396 indicates better growth in the population inhabiting waste land (RYK). Roots, being underground
397 plant parts, are relatively less affected by environmental conditions compared to other plant organs
398 (Fitter and Hay, 2012). Epidermis is an outermost protective layer of roots, and under harsh
399 condition it strong friction of rhizospheric soil (McKenzie et al., 2013). In resulting, this may be
400 damaged, mainly in grasses and herbs (McCully, 1999). *P. hysterothorus* showed a significant
401 increase of this parameter in MUL population (along water channel). Thicker epidermal layers
402 play vital role in resisting the friction of soil compaction as well as impede the excessive water
403 and solute translocation inside root tissues (Chimungu et al., 2015). The water storage parenchyma
404 (cortex) and vascular region (metaxylem vessels and phloem) in the roots play a crucial role,
405 especially during water deficit or saline conditions. These adaptations are particularly significant
406 for the survival of arid zone species such as *P. hysterothorus* (Hsiao and Xu, 2000). A significantly
407 increased storage parenchyma and vascular region has been observed in populations of KHP (along
408 waste deposit) and MUZ (along agriculture field).

409 The plants growing in wastelands (KHP) demonstrated the highest values for the majority of stem
410 anatomical characteristics, as shown in Table 4. These characteristics encompass dermal, vascular,
411 and storage tissues, indicating favorable growth conditions and enhanced biomass production, as
412 evidenced by the shoot fresh weight (Table 4). These findings are consistent with previous studies
413 conducted by Engloner (2009) and Guo and Miao (2010). The presence of sclerified tissues in the
414 stems is a notable adaptation to dry conditions (Nikolova and Vassilev, 2011). It was recorded in
415 stems from almost all habitats, but in populations from roadsides (VEH and DGK), there was
416 higher lignin deposition compared to the other populations. Under extreme dry and hot condition,
417 tissue sclerification is beneficial for preventing from collapse of internally metabolically active
418 tissues during desiccation (Ahmad et al., 2016; da Cruz Maciel et al., 2015).

419 In arid zone species like *P. hysterothorus*, the leaf blade plays a vital role as it needs to withstand
420 harsh environmental conditions for the plant's survival. Among the studied populations, the plants
421 from roadside habitats (VEH) exhibited the highest values for various leaf anatomical
422 characteristics, including leaf thickness in terms of midrib and lamina thickness, as well as
423 mechanical and storage tissues such as cortical thickness and its cells area. These adaptations are
424 indicative of the plant's ability to protect the leaf blade from the challenging environmental
425 conditions encountered in roadside habitats. Three populations namely KHP (near wasteland),

426 AHP and LAP (along agriculture field) possessed thick epidermis and spare surface hairiness. Both
427 are effective for evapo-transpiration loss when population surviving in dry environmental
428 condition (González et al., 2008).

429 **Conclusion**

430 In conclusion, *P. hysterophorus* displays significant variations in both structural and functional
431 attributes, enabling it to tolerate diverse environmental adversities. The wide distribution of this
432 species can be attributed to its specific adaptations along environmental gradients. It exhibits a
433 range of adaptations, including changes in growth parameters, microstructural features, and
434 functional traits. These adaptations, such as enhanced biomass production, long and numerous
435 roots, thicker epidermis, development of storage parenchyma tissues, lignification of cortical
436 region and vascular bundles, and increased levels of organic osmolytes and antioxidants. Overall,
437 the structural and functional adaptations of *P. hysterophorus* contribute to its resilience,
438 competitive ability, and ability to colonize a wide range of habitats, making it a successful and
439 problematic invasive species.

440 **Acknowledgements:** The content of this manuscript has been derived from the MPhil Thesis of
441 the second author.

442 **Author Contribution:**

443 ZU: The principal researcher responsible for conducting the experimental work.

444 UI: The principal supervisor of the second author, providing guidance in statistical analysis, data
445 visualization, modeling, and interpretation.

446 UI and KSA: Conducted a thorough review of the article to correct any language errors.

447 AA and HA: Contributed to the research by carrying out the practical aspects, including
448 biochemical analysis, anatomical photography, and data collection.

449 **Availability of Data and Material:**

450 All the data and relevant information is present in the manuscript.

451 **Declarations**

452 **Ethics Approval:** Since the study did not involve animal or human subjects, specific ethical
453 approval was not required. However, all necessary guidelines provided by The Islamia University
454 of Bahawalpur, Rahim Yar Khan Campus for handling plant material in the laboratory were strictly
455 adhered to. Following the completion of the study, proper measures were taken to dispose of all
456 materials in order to prevent any potential bio-contamination.

457 **Consent to Participate:** The contributions of all participants in this study have been duly
458 recognized and acknowledged. Each participant has been listed as an author or included in the
459 acknowledgements section to acknowledge their respective roles and contributions to the research.

460 **References**

461 Abideen, Z., H.W. Koyro, B. Huchzermeyer, R. Ansari, F. Zulfiqar and B. Gul. 2019.
462 Ameliorating effects of biochar on photosynthetic efficiency and antioxidant defense of
463 *Phragmites karka* under drought stress. Plant Biology. doi:10.1111/plb.13054.

464 Adkins, S., & Shabbir, A. (2014). Biology, ecology and management of the invasive parthenium
465 weed (*Parthenium hysterophorus* L.). Pest management science, 70(7), 1023-1029.

466 Ahmad, K.S., Hameed, M., Deng, J., Ashraf, M., Hamid, A., Ahmad, F., Fatima, S., Akhtar, N.,
467 2016. Ecotypic adaptations in Bermuda grass (*Cynodon dactylon*) for altitudinal stress tolerance.
468 Biologia 71, 885–895.

469 Ali, Z., M. Ashraf, M.Y. Ashraf, S. Anwar and K. Ahmad. 2020. Physiological response of
470 different accessions of *Sesbania sesban* and *Cyamopsis tetragonoloba* under water deficit
471 conditions. Pak. J. Bot., 52(2): DOI: [http://dx.doi.org/10.30848/PJB20202\(43\)](http://dx.doi.org/10.30848/PJB20202(43)).

472 Almohisen, I.A.A. 2014. Response of free amino acids in four legumes plants to air pollution. J.
473 Biol. Today's World, 3(8): 169-173.

474 Alvarez Flores, R., A. Nguyen Thi Truc, S. Peredo Parada, R. Joffre and T. Winkel. 2018. Rooting
475 plasticity in wild and cultivated Andean *Chenopodium* species under soil water deficit. Plant Soil.,
476 425: 479-492.

477 Alvarez, J.M., J.F. Rocha and S.R. Machado, 2008. Bulliform cells in *Loudetiopsis chrysothrix*
478 (Nees) Conert and *Tristachya leiostachya* Nees (Poaceae): structure in relation to function. Braz.
479 Arch. Biol. Technol., 51: 113–119.

480 Amirjani, M.R. 2011. Effect of salinity stress on growth, sugar content, pigments and enzyme
481 activity of rice. Int. J. Bot., 7: 73-81.

482 Ann. Rev. Plant Biol. 50, 695–718.

483 Arnon DI (1949). Copper enzymes in isolated chloroplasts polyphenoloxidase in *Beta vulgaris*.
484 Plant Physiol 24:1–15.

- 485 Bates LS, Waldren RP, Teare ID. 1973. Rapid determination of proline for water stress studies.
486 Plant Soil 39: 205–207. DOI: 10.1007/BF00018060.
- 487 Boughalleb, F., R. Abdellaoui, N. Ben Brahim and M. Neffati. 2014. Anatomical adaptations of
488 *Astragalus gombiformis* Pomel. under drought stress. Open Life. Sci., 9: 1215–1225.
- 489 Caemmerer, S., Evans, J.R., 2015. Temperature responses of mesophyll conductance differ greatly
490 between species. Plant Cell Environ. 38, 629–637.
- 491 Chattopadhyay, A., P. Subba, A. Pandey, D. Bhushan, R. Kumar, A. Datta, S. Chakraborty and N.
492 Chakraborty. 2011. Analysis of the grass pea proteome and identification of stress-responsive
493 proteins upon exposure to high salinity, low temperature, and abscisic acid treatment. Phytochem.,
494 72: 1293–1307.
- 495 Chimungu, J.G., Loades, K.W., Lynch, J.P., 2015. Root anatomical phenes predict root penetration
496 ability and biomechanical properties in maize (*Zea mays*). J. Exp. Bot. 66, 3151–3162.
- 497 da Cruz Maciel, J.R., de Oliveira, D., Fadin, D.A., das Graças Sajo, M., Pedroso-de-Moraes, C.,
498 2015. Morpho-anatomical characteristics conferring drought tolerance in roots of sugar cane
499 genotypes (*Saccharum* L., Poaceae). Braz. J. Bot. 38, 951–960.
- 500 Davis BH (1979). Chemistry and Biochemistry of Plant Pigments, 2nd edn, pp:149–155. Godwin
501 TW (Ed.). Academic Press Inc., London.
- 502 De Micco, V., Aronne, G., 2012. Morpho-anatomical traits for plant adaptation to drought. Plant
503 Responses to Drought Stress. Springer, Berlin Heidelberg, pp. 37–61.
- 504 El Afry, M.M., M.M.F, El Nady and E. B. Abdelmonteleb. 2012. Anatomical studies on drought
505 stressed wheat plants (*Triticum aestivum* L.) treated with some bacterial strains. Acta. Biol.
506 Szeged., 56: 165–174.
- 507 Engloner, A.I., 2009. Structure, growth dynamics and biomass of reed (*Phragmites australis*)—a
508 review. Flora 204, 331–346.
- 509 Fitter, A.H., Hay, R.K., 2012. Environmental Physiology of Plants. Academic Press.

- 510 Gonzáles, W.L., Negritto, M.A., Suárez, L.H., Gianoli, E., 2008. Induction of glandular and non-
511 glandular trichomes by damage in leaves of *Madia sativa* under contrasting water regimes. *Acta*
512 *Oecol.* 33, 128–132.
- 513 Grattan SR, Grieve CM. 1998. Salinity-mineral nutrient relations in horticultural crops. *Scientia*
514 *Horticulturae* 78: 127-57. DOI: 10.1016/S0304-4238(98)00192-7.
- 515 Guo, Z.H., Miao, X.F., 2010. Growth changes and tissues anatomical characteristics of giant reed
516 (*Arundo donax* L.) in soil contaminated with arsenic, cadmium and lead. *J. Cent. S. Univ. Technol.*
517 17, 770–777.
- 518 Hameed, M., Ashraf, M., & Naz, N. (2009). Anatomical adaptations to salinity in cogon grass
519 [*Imperata cylindrica* (L.) Raeuschel] from the Salt Range, Pakistan. *Plant and soil*, 322(1), 229-
520 238.
- 521 Hameed, M., Ashraf, M., & Naz, N. (2011). Anatomical and physiological characteristics relating
522 to ionic relations in some salt tolerant grasses from the Salt Range, Pakistan. *Acta Physiologiae*
523 *Plantarum*, 33(4), 1399-1409.
- 524 Hamza, M.A. and W.K. Anderson. 2005. Soil compaction in cropping systems: A review of the
525 nature, causes and possible solutions. *Soil Tillage Res.*, 82: 121-145.
- 526 Hasanuzzaman, M., K. Nahar, M.M. Alam, P.C. Bhowmik, M.A. Hossain, M.M. Rahman, M.N.
527 V. Prasad, M. Ozturk and M. Fujita. 2014. Potential use of halophytes to remediate saline soils.
528 *BioMed Res. Int.*, 2014: 1-12.
- 529 Hsiao, T.C., Xu, L.K., 2000. Sensitivity of growth of roots versus leaves to water stress:
530 biophysical analysis and relation to water transport. *J. Exp. Bot.* 51, 1595–1616.
- 531 Kholodova, V., Volkov, K., & Kuznetsov, V. (2010). Plants under heavy metal stress in saline
532 environments. In *Soil heavy metals* (pp. 163-183). Springer, Berlin, Heidelberg.
- 533 Khosroshahi, M.Z., M.E. Ashari, A. Ershadi and A. Imani. 2014. Morphological changes in
534 response to drought stress in cultivated and wild almond species. *Int. J. Hort. Sci. Tech.*, 1(1): 79-
535 92.

- 536 Leukovic, J., I. Maksimovic, L. Zoric, N. Negl, M. Percic, D. Polic and M. Putnic delic. 2009.
537 Histological characteristics of sugar beet leaves potentially linked to drought tolerance. *Ind. Crop.*
538 *Prod.*, 30: 281-86.
- 539 Lopes, D.M., N. Walford, H. Viana and C.R.S. Junior. 2016. A proposed methodology for the
540 correction of the leaf area index measured with a ceptometer for *Pinus* and *Eucalyptus* forests.
541 *Revista Arvore*, Viçosa-MG, 40: 845-854.
- 542 López-Millán, A. F., Sagardoy, R., Solanas, M., Abadía, A., & Abadía, J. (2009). Cadmium
543 toxicity in tomato (*Lycopersicon esculentum*) plants grown in hydroponics. *Environmental and*
544 *experimental botany*, 65(2-3), 376-385.
- 545 Lowry RJ, Rosenbrough NJ, Farr AL, Randall RJ. 1951. Protein measurement with the folin
546 reagent. *Journal of Biological Chemistry* 193: 265–275.
- 547 Maharjan, S., Shrestha, B. B., Devkota, A., Muniappan, R., & Jha, P. K. (2020). Temporal and
548 spatial patterns of research on a globally significant invasive weed *Parthenium hysterophorus* L.:
549 A bibliographic review. *Crop Protection*, 135, 104832.
- 550 Makbul, S., N. Suhan Güler, N. Durmuş and S. Güven. 2011. Changes in anatomical and
551 physiological parameters of soybean under drought stress. *Turk. J. Bot.*, 35: 369-77.
- 552 McCully, M.E., 1999. Roots in soil: unearthing the complexities of roots and their rhizospheres.
- 553 McGeoch, M. A., Butchart, S. H., Spear, D., Marais, E., Kleynhans, E. J., Symes, A., ... &
554 Hoffmann, M. (2010). Global indicators of biological invasion: species numbers, biodiversity
555 impact and policy responses. *Diversity and Distributions*, 16(1), 95-108.
- 556 McKenzie, B.M., Mullins, C.E., Tisdall, J.M., Bengough, A., 2013. Root-soil friction:
557 quantification provides evidence for measurable benefits for manipulation of root-tip traits. *Plant*
558 *Cell Environ.* 36, 1085–1092.
- 559 Medranoa, H., M. Tomás, S. Martorella, J. Flexasa, E. Hernández, J. Rosselló, A. Poub, J.
560 Escalona and J. Bota. 2015. From leaf to whole-plant water use efficiency (WUE) in complex
561 canopies: Limitations of leaf WUE as a selection target. *Crop J.*, 3: 220-228.

- 562 Micco, V.D. and G. Aronne, 2012. Occurrence of morphological and anatomical adaptive traits in
563 young and adult plants of the rare Mediterranean Cliff species *Primula palinuri* Petagna. Sci.
564 World J., 2012: 1–10.
- 565 Mohrs, C.F. 1856. New mass analytical determination of chlorine in compounds translates. Ann.
566 Chem. Pharm., 97: 335-338.
- 567 Mojica, J.P., Y.W. Lee, J.H. Willis and J.K. Kelly. 2012. Spatially and temporally varying
568 selection on intrapopulation quantitative trait loci for a life history trade-off in *Mimulus guttatus*.
569 Mol. Ecol., 21: 3718-3728.
- 570 Nadgorska-Socha, A., B. Ptasinska and A. Kita. 2013. Heavy metal bioaccumulation and
571 antioxidative responses in *Cardaminopsis arenosa* and *Plantago lanceolata* leaves from
572 metalliferous and non-metalliferous sites: a field study. Ecotoxicol., 22(9): 1422-1434.
- 573 Nikolova, A., Vassilev, A., 2011. A study on *Tribulus terrestris* L. anatomy and ecological
574 adaptation. Biotechnol. Biotechnol. Equip. 25, 2369–2372.
- 575 Oliveira, I., A. Meyer, S. Afonso and B. Gonçalves. 2018. Compared leaf anatomy and water
576 relations of commercial and traditional *Prunus dulcis* (Mill.) cultivars under rain fed conditions.
577 Sci. Hort. Amsterdam., 229: 226-232.
- 578 Paccard A., M. Vance and Y. Willi. 2013. Weak impact of fine-scale landscape heterogeneity on
579 evolutionary potential in *Arabidopsis lyrata*. J. Evol. Biol., 26: 2331-2340.
- 580 Peng, H., Kroneck, P. M., & Küpper, H. (2013). Toxicity and deficiency of copper in *Elsholtzia*
581 *splendens* affect photosynthesis biophysics, pigments and metal accumulation. Environmental
582 science & technology, 47(12), 6120-6128.
- 583 Qadir, M., A. Tubeileh, J. Akhtar, A. Larbi, P.S. Minhas and M.A. Khan. 2008. Productivity
584 enhancement of salt-affected environments through crop diversification. Land Degrad. Develop.,
585 19: 429-453.
- 586 Rahmat, A., V. Kumar, L.M. Fong, S. Endrini and H.A. Sani. 2003. Determination of total
587 antioxidant activity in three types of local vegetables shoots and the cytotoxic effect of their
588 ethanolic extracts against different cancer cell lines. Asia Pac. J. Clin. Nutr., 12(3): 308-311.

- 589 Ruzin SE (1999) Plant Microtechnique and Microscopy. Oxford University Press, New York, NY,
590 USA.
- 591 Sarabi, B., S. Bolandnazar, N. Ghaderi and J. Ghashghaie. 2017. Genotypic differences in
592 physiological and biochemical responses to salinity stress in melon (*Cucumis melo* L.) plants:
593 prospects for selection of salt tolerant landraces. *Plant Physiol. Biochem.*, 119: 294-311.
- 594 Sharma, S.S. and K. Dietz. 2006. The significance of amino acids and amino acid-derived
595 molecules in plant responses and adaptation to heavy metal stress. *J. Exp. Bot.*, 57(4): 711-726.
- 596 Siringam, K., Juntawong, N., Cha-um, S., & Kirdmanee, C. (2011). Salt stress induced ion
597 accumulation, ion homeostasis, membrane injury and sugar contents in salt-sensitive rice (*Oryza*
598 *sativa* L. spp. indica) roots under isoosmotic conditions. *African Journal of Biotechnology*, 10(8),
599 1340-1346.
- 600 Sun, M., H.H. Chen, J.P. Xu, H.T. Yue and K. Tian, 2018. Evolutionary associations of leaf
601 functional traits in nine Euphorbiaceae species. *Intl. J. Agric. Biol.*, 20: 1309–1317.
- 602 Sun, Y., Fan, X. Y., Cao, D. M., Tang, W., He, K., Zhu, J. Y., ... & Wang, Z. Y. (2010). Integration
603 of brassinosteroid signal transduction with the transcription network for plant growth regulation
604 in *Arabidopsis*. *Developmental cell*, 19(5), 765-777.
- 605 Sytar, O., Kumar, A., Latowski, D., Kuczynska, P., Strzałka, K., & Prasad, M. N. V. (2013). Heavy
606 metal-induced oxidative damage, defense reactions, and detoxification mechanisms in plants. *Acta*
607 *physiologiae plantarum*, 35(4), 985-999.
- 608 Talukdar, D. 2013. Comparative morpho-physiological and biochemical responses of lentil and
609 grass pea genotypes under water stress. *J. Nat. Sci. Biol. Med.*, 4(2): 396-402.
- 610 Walkley, A. 1947. A critical examination of a rapid method for determining organic carbon in
611 soils: effect of variations in digestion conditions and of inorganic soil constituents. *Soil Sci.*, 63:
612 251-264.
- 613 Weraduwege, S.M., J. Chen, F.C. Anozie, A. Morales, S.E. Weise and T.D. Sharkey. 2015. The
614 relationship between leaf area growth and biomass accumulation in *Arabidopsis thaliana*. *Front*
615 *Plant Sci.*, 6: 167.

- 616 Wolf, B. 1982. A comprehensive system of leaf analysis and its use for diagnosing crop nutrient
617 status. *Comm. Soil Sci. Plant Anal.*, 13: 1035-1059.
- 618 Ye, T., H. Shi, Y. Wang and Z. Chan. 2015. Contrasting changes caused by drought and
619 submergence stresses in bermuda grass (*Cynodon dactylon*). *Front. Plant Sci.*, 6: 1-14.
- 620 Zemanova, V., M. Pavlik, D. Pavlikova and P. Tlustos. 2013. The changes of contents of selected
621 free amino acids associated with cadmium stress in *Noccaea caerulea* and *Arabidopsis halleri*.
622 *Plant Soil Environ.*, 59(9): 417-422.
- 623 Zulfiqar, F., A. Casadesús, H. Brockman, and S. Munné Bosch. 2019a. An overview of plant based
624 natural biostimulants for sustainable horticulture with a particular focus on *Moringa* leaf extracts.
625 *Plant Sci.*, 110194.
- 626 Zulfiqar, F., N.A. Akram and M. Ashraf. 2020. Osmoprotection in plants under abiotic stresses:
627 new insights into a classical phenomenon. *Planta.*, 251(1): 3.

Table 1 (on next page)

Table 1. Metrological record of differently adapted populations of star weed (*Parthenium hysterophorus* L.) collected from Punjab province

1 **Table 1. Metrological record of differently adapted populations of star weed (*Parthenium hysterophorus* L.) collected from**
 2 **Punjab province**

Ecological regions	Collection sites	Habitat types	Annual Temp. (°C)		Rainfall (mm)	Altitude m.a.s.l	Longitude (N)	Latitude (E)
			Max.	Min.				
Near wasteland	Rahim Yar Khan	Near the wasteland	44	13	115	88	28° 42' 12.29"	70° 29' 89.19"
	Sadiqabad	Along barren land	40	12	101	76	28° 09' 19.29"	70° 19' 12.99"
	Khanpur	Near waste deposit	43	15	410	184	32° 08' 51.27"	72° 38' 30.22"
Along water channel	Bahawalpur	Along the river Indus	44	13	679	149	31° 08' 41.23"	72° 08' 46.38"
	Liaquatpur	Along the water canal	34	14	519	237	32° 43' 19.02"	72° 58' 42.73"
	Ahmadpur	Near Punjab barrage	40	16	842	212	30° 39' 31.63"	73° 23' 50.62"
	Multan	Along Chenab River	38	12	609	186	32° 17' 43.54"	72° 21' 03.24"
Along roadside	Vehari	Near the roadside	41	12	195	146	30° 55' 46.74"	71° 45' 41.90"
	DG Khan	Along railway track	40	11	143	198	28° 27' 42.58"	71° 03' 919.22"
	Rajanpur	Near M5 motorway	43	12	120	117	28° 46' 04.86"	71° 20' 03.13"
	Jhang	Near GT road	40	10	155	267	29° 58' 01.03"	70° 19' 36.63"
Near agriculture field	Muzaffargarh	Near cotton field	44	13	576	210	32° 25' 30.62"	37° 13' 31.40"
	Sargodha	Along sorghum field	38	9	346	192	31° 28' 42.68"	73° 12' 36.66"
	Faisalabad	Along Rice field	40	8	200	140	29° 20' 05.33"	71° 56' 04.29"
	Layyah	Wheat field	43	12	400	288	32° 24' 45.54"	71° 58' 00.51"

3

4

Table 2 (on next page)

Soil physicochemical parameters of collection sites of differently adapted populations of star weed (*Parthenium hysterophorus* L.) collected from Punjab province

1 **Table 2. Soil physicochemical parameters of collection sites of differently adapted populations of star weed (*Parthenium***
 2 ***hysterophorus* L.) collected from Punjab province**

Ecological regions	Collection sites	Soil texture	ECe (dS m ⁻¹)	pH	OM (%)	SP (%)	PO ₄ ³⁻ (mg L ⁻¹)	NO ₃ ⁻ (mg L ⁻¹)	Cl ⁻ (mg L ⁻¹)	Ca ²⁺ (mg L ⁻¹)	Na ⁺ (mg L ⁻¹)	K ⁺ (mg L ⁻¹)
Near wasteland	RYK	Loamy	6.73a	6.2j	0.35e	36c	3.1b	3.3c	567.8a	156.1a	398.9a	64.4j
	SDK	Sandy	0.76h	8.4g	0.42d	16gh	1.6g	2.9d	83.4h	54.2g	54.2i	70.1i
	KHP	Loamy	6.69a	8.8b	0.28g	38b	3.4ab	4.0b	434.5b	67.7ef	297.1b	260.3b
Along water channel	BWP	Sandy	0.96g	8.7c	0.28g	17gh	1.9d	2.9d	102.7g	71.9e	147.8f	80.8g
	LAP	Sandy	3.46c	8.0h	0.35e	15h	2.2c	3.2c	389.1c	97.3c	297.1b	180.9d
	AHP	Sandy	1.06f	8.6d	0.42d	16gh	1.9d	3.5c	130.5f	63.5f	164.1e	148.5e
	MUL	Loamy sand	4.33b	7.8i	0.56a	22d	2.2c	3.2c	72.1j	60.2f	266.1c	276.3a
Along roadside	VEH	Loamy	1.15e	8.2f	0.21h	32d	3.1b	4.3b	109.8g	78.7d	180.7d	124.1f
	MUZ	Sandy	1.33d	8.2f	0.28g	17gh	1.9d	2.0e	178.6e	110.9b	134.0	80.1g
	SAR	Sandy	0.77h	8.5e	0.45b	18f	1.9d	4.0b	79.6i	77.1d	175.0d	75.2h
	FSD	Sandy	1.08f	8.7c	0.43bd	19e	2.3c	4.0b	111.6g	104.3bc	147.1f	196.6c
Near agriculture field	DGK	Clayey loam	1.19e	8.7b	0.28g	38b	3.4ab	4.0b	71.1j	66.7ef	60.8h	258.3b
	RJP	Loamy sand	0.90g	8.5e	0.26g	16gh	1.8d	2.8d	100.7g	70.9e	145.8f	79.8g
	JHG	Loamy	3.01c	8.0h	0.35e	15h	2.2c	3.2c	389.1c	97.3c	61.8h	180.9d
	RYK	Loamy	1.20de	8.9a	0.3f	42a	3.6a	5.1a	198.3d	94.3c	88.9g	276.8a
	LSD		0.5	1.0	0.5	6.0	0.5	1.0	7.0	6.0	25.8	6.0

3 Means shearing similar letter in each row are not statistically significant.

4 * = Significant at $P < 0.05$, ** = Significant at $P < 0.01$, *** = Significant at $P < 0.001$, NS = not significant

5 **Abbreviations are given as footnote of figure 7.**

6

7

8

Table 3(on next page)

Growth and physiological attributes of differently adapted populations of star weed (*Parthenium hysterophorus* L.) collected from Punjab province

Abbreviations are given at start of manuscript. Means shearing similar letters in each row are statistically not significant *, significant at $P < 0.05$; **, significant at $P < 0.01$; ***, significant at $P < 0.001$; NS, not significant

1 **Table 3. Growth and physiological attributes of differently adapted populations of star weed (*Parthenium hysterophorus* L.)**
 2 **collected from Punjab province**

Ecological regions	Near wasteland			Along water channel				Along roadside				Near ariculture field					
Collection sites	RYK	SDA	KHP	BWP	LAP	AHP	MUL	VEH	DGK	RJP	JHG	MUZ	SAR	FSD	LYH	LSD	F-value
Growth attributes																	
Plant height (cm)	37.0d	46.0b	40.3c	56.5a	45.0b	31.0e	39.5c	41.2c	37.3d	20.3f	37.7d	36.3d	43.0c	16.3g	30.0e	11.6	72.6***
Shoot length (cm)	30.0d	40.3b	31.0d	44.7a	35.0c	26.0e	33.0cd	36.3c	30.4d	16.3f	28.0d	30.0d	33.0cd	11.3g	24.0e	4.5	19.4***
Shoot fresh weight (g plant ⁻¹)	6.3d	8.2bc	11.5a	9.4b	8.2bc	5.4de	7.7c	11.0a	4.5e	4.5e	9.4b	4.7e	11.5a	3.0f	4.4de	2.2	14.9***
Shoot dry weight (g plant ⁻¹)	3.1c	4.1b	5.8a	4.7b	4.1b	2.7cd	3.9b	5.6a	2.2d	2.0d	4.7b	2.3d	5.8a	1.2e	2.0cd	1.4	11.8**
Root length (cm)	8.0b	6.0c	8.0b	11.5a	10.0ab	7.7b	5.7c	4.5d	7.3bc	7.7b	10.0ab	6.0c	10.0ab	6.0c	7.2b	1.8	31.7***
Root fresh weight (g plant ⁻¹)	1.5a	0.5bc	1.5a	0.7b	1.4a	0.6c	0.7b	0.7b	0.7b	0.4d	0.6c	0.8b	1.5a	0.5bc	0.5c	1.0	68.8***
Root dry weight (g plant ⁻¹)	1.2a	0.3e	1.0ab	0.2f	1.0ab	0.2f	0.3e	0.4d	0.5c	0.2f	0.3e	0.5c	1.0ab	0.3e	0.1f	0.5	86.1***
Leaf number (per branch)	29.5a	18.5d	25.5b	17.0d	19.0d	10.5ef	14.0e	22.0c	15.5e	14.5e	18.5d	11.0ef	20.5c	9.0f	9.5ef	4.3	25.7***
Leaf area (cm ²)	14.9i	53.4c	19.2	65.2a	38.4e	39.2e	23.9	65.4a	38.0e	16.6h	27.6g	47.9d	59.3b	33.7f	37.2e	9.8	8.3**
Physiological attributes																	
Total soluble protein (µg g ⁻¹ d.wt.)	47.9a	26.4f	21.7g	41.9b	20.8g	23.1g	22.8g	9.4i	32.0d	29.8e	35.7c	19.3h	36.3c	24.7g	22.1g	6.7	33.3***
Proline (µmol g ⁻¹ dwt.)	8.8c	8.8c	7.0d	19.8a	5.9e	1.6g	3.5f	3.6f	6.7de	10.4b	10.8b	8.9c	7.9c	8.5c	1.6g	9.1	39.1***
Glycine betaine (µmol g ⁻¹ dwt.)	3.6b	3.8b	2.6c	10.2a	2.2c	2.5c	2.4c	2.1c	2.4c	3.1b	2.4c	2.6c	3.9b	1.9d	2.3c	4.5	35.0***
Chlorophyll a (mg g ⁻¹ f. wt.)	1.9c	2.4a	1.9c	1.9c	1.7cd	2.2b	1.3d	1.7cd	1.3d	1.3d	1.3d	1.7cd	2.2b	1.3d	2.0b	1.3	52.8***
Chlorophyll b (mg g ⁻¹ f. wt.)	0.3f	2.0a	0.7e	1.8ab	1.0d	1.7ab	1.8ab	1.8ab	0.8e	1.5c	2.0a	2.0a	1.3c	2.0a	1.6ab	1.0	40.2***
Total chlorophyll (mg g ⁻¹ f. wt.)	2.2f	4.4a	2.6d	3.7ab	2.7d	3.9ab	3.1c	3.5b	2.1f	2.8e	3.3b	3.7ab	3.5b	3.3b	3.7ab	1.5	60.5***
Carotenoids (mg g ⁻¹ f. wt.)	1.5d	2.4b	1.4d	1.4d	2.8a	1.8c	1.8c	2.6ab	1.8c	1.7c	1.9c	1.0e	2.5b	1.7c	1.6c	1.1	18.8***
Chlorophyll a/b	6.3a	1.2d	2.7b	1.0e	1.7c	1.2d	0.7f	0.9f	1.6c	0.8f	0.6g	0.8f	0.3h	0.6g	1.0d	0.5	73.1***
Total Chlorophyll/Carotenoid	1.4e	3.1ab	1.0f	2.6c	1.3e	0.9g	1.7d	0.3h	1.1f	1.6d	1.7d	3.7a	1.4e	1.9d	0.7g	0.9	89.2***
Antioxidant activity (%)	5.0d	5.4d	4.2e	5.2d	3.5f	6.5c	9.9a	9.9a	9.9a	6.1c	9.3ab	5.7	6.2c	7.8bc	6.4c	3.3	36.4***

3 Abbreviations are given at start of manuscript. Means shearing similar letters in each row are statistically not significant

4 *, significant at $P < 0.05$; **, significant at $P < 0.01$; ***, significant at $P < 0.001$; NS, not significant

5 Abbreviations are given as footnote of figure 7.

6

7

8

Table 4(on next page)

Anatomical characteristics of differently adapted populations of star weed (*Parthenium hysterophorus* L.) collected from Punjab province

Abbreviations are given at the start of manuscript. Means shearing similar letters in each row are statistically not significant. *, significant at $P < 0.05$; **, significant at $P < 0.01$; ***, significant at $P < 0.001$; NS, not significant

1 **Table 4. Anatomical characteristics of differently adapted populations of star weed (*Parthenium hysterophorus* L.) collected**
 2 **from Punjab province**

Ecological regions	Near wasteland			Along water channel				Along roadside				Near ariculture field				LSD	F-ratio
Collection sites	RYK	SDA	KHP	BWP	LAP	AHP	MUL	VEH	DGK	RJP	JHG	MUZ	SAR	FSD	LYH	LSD	F-ratio
Root anatomy																	
Root area (µm ²)	400.4a	282.6e	259.1f	259.1f	306.2d	304.6d	306.2d	306.2d	353.3b	329.7c	282.6h	329.7c	400.4a	259.1g	353.3b	10.9	66.5***
Epidermal thickness (µm)	18.8c	17.3c	12.6de	18.8c	22.0b	17.3c	31.4a	17.3c	14.1d	15.7d	22.0b	15.7d	22.0b	14.1d	9.4e	5.4	47.3***
Cortical thickness (µm)	94.2a	37.7e	51.8d	45.5d	55.0c	37.7e	55.0c	65.9b	55.0c	67.5b	55.0c	36.1e	55.0c	31.4f	65.9b	8.9	98.6***
Cortical cell area (µm ²)	14.1a	9.4c	14.1a	11.0b	9.4c	9.4c	9.4c	11.0b	9.4c	9.4c	9.4c	7.4d	7.4d	9.4c	9.4c	2.5	86.4***
Vascular bundle areas (µm ²)	70.7c	94.2b	70.7c	121.3a	69.1e	94.2b	55.0e	70.7c	65.9	67.5d	70.7c	70.7c	67.5d	70.7c	69.1c	20.3	72.4***
Metaxylem area (µm ²)	12.6c	11.0d	15.7a	15.7a	12.6c	11.0d	12.6c	9.4e	12.6c	11.0d	14.1b	15.7a	9.4e	12.6c	14.1b	4.3	85.8***
Phloem area (µm ²)	1.0c	1.8b	2.5a	0.5d	2.5a	1.9b	1.8b	1.0c	1.0c	1.9b	0.5d	2.6a	1.7b	2.6a	1.9b	1.1	19.9***
Stem anatomy																	71.6***
Stem area (µm ²)	229.1g	282.6e	440.4a	259.1f	290.2d	290.6d	290.2d	290.2d	343.3b	300.7c	182.6h	440.4a	259.1f	300.7c	340.3b	32.2	35.6***
Epidermal thickness (µm)	9.4d	14.1c	23.6a	14.1c	14.1c	18.8b	9.4d	18.8b	14.1c	9.4d	14.1c	9.4	23.6a	14.1c	14.1c	6.5	6.5
Cortical thickness (µm)	18.8h	23.6g	70.7a	33.0f	55.0c	47.1d	18.8h	47.1d	67.5ab	47.1d	47.1d	39.3e	59.7b	47.1d	47.1d	12.4	37.6***
Cortical cell area (µm ²)	12.6b	9.4c	11.9b	6.3d	14.1a	9.4c	9.4c	9.4c	11.0b	9.4c	11.0b	9.4c	9.4c	14.1a	14.1a	3.1	19.5***
Vascular bundle area (µm ²)	94.2h	94.2h	164.2h	131.9e	108.3g	164.9a	146.0c	117.8f	146.0c	149.2b	128.7e	117.8f	133.5d	94.2h	133.5d	12.7	49.4***
Metaxylem area (µm ²)	12.6bc	15.7b	17.3a	9.4c	14.1b	14.1b	18.8a	9.4c	14.1b	14.1b	14.1b	9.4c	14.1b	14.1b	9.4c	4.4	87.3***
Phloem area (µm ²)	20.4f	14.1g	36.1e	40.8d	47.1c	48.7c	45.5c	47.1c	58.1b	47.1c	47.1c	42.4d	47.1c	58.1b	69.1a	15.8	52.3***
Leaf anatomy																	57.8***
Midrib thickness (µm)	379.9c	420.8a	376.8c	337.6d	329.7e	235.5d	329.7e	389.4b	376.8c	329.7e	329.7e	329.7e	282.6f	235.5g	282.6f	12.9	18.5***
Lamina thickness (µm)	22.0c	14.1e	18.8d	14.1e	22.0c	17.3d	18.8d	38.1a	17.3d	11.0f	14.1e	14.1e	28.3b	26.7bc	14.1e	6.4	73.8***
Epidermal thickness (µm)	18.8b	15.7c	22.0a	14.1d	22.0a	23.6a	10.6e	15.7c	14.1c	12.6	17.3b	17.3b	15.7c	18.8b	15.7c	3.3	89.4***
Cortical thickness (µm)	117.8h	106.8i	141.3e	180.6ab	139.7	117.8h	150.7d	185.3a	153.9d	158.6c	127.2g	122.5g	139.7f	100.1j	119.3h	17.6	36.3***
Cortical cell area (µm ²)	14.1b	14.1b	15.7b	15.7b	12.6c	11.0c	15.7b	18.8a	11.0c	14.1b	14.1b	18.8a	14.1b	9.4d	9.4d	4.4	72.7***
Vascular bundle area (µm ²)	47.1f	117.8a	92.6c	83.2d	70.7e	69.1e	69.1e	70.7e	83.2d	97.3b	69.1e	92.6c	70.7e	70.7e	83.2d	12.5	19.8***
Metaxylem area (µm ²)	18.8e	37.7a	29.8b	10.9g	17.3e	16.2ef	11.8	22.0d	22.0d	20.4e	25.1c	17.3e	18.8e	14.1f	22.0d	8.0	14.5**
Phloem area (µm ²)	15.7c	23.6b	11.8d	16.0c	14.1c	12.2d	16.0c	20.4bc	20.4bc	22.0bc	23.6b	20.4bc	28.3a	15.7c	20.4bc	5.2	11.3**

3 Abbreviations are given at the start of manuscript. Means shearing similar letters in each row are statistically not significant.

4 *, significant at $P < 0.05$; **, significant at $P < 0.01$; ***, significant at $P < 0.001$; NS, not significant

5 Abbreviations are given as footnote of figure 7.

6

Figure 1

Map of Punjab showing collection sites of *Parthenium hysterophorus* L. sampled from different districts

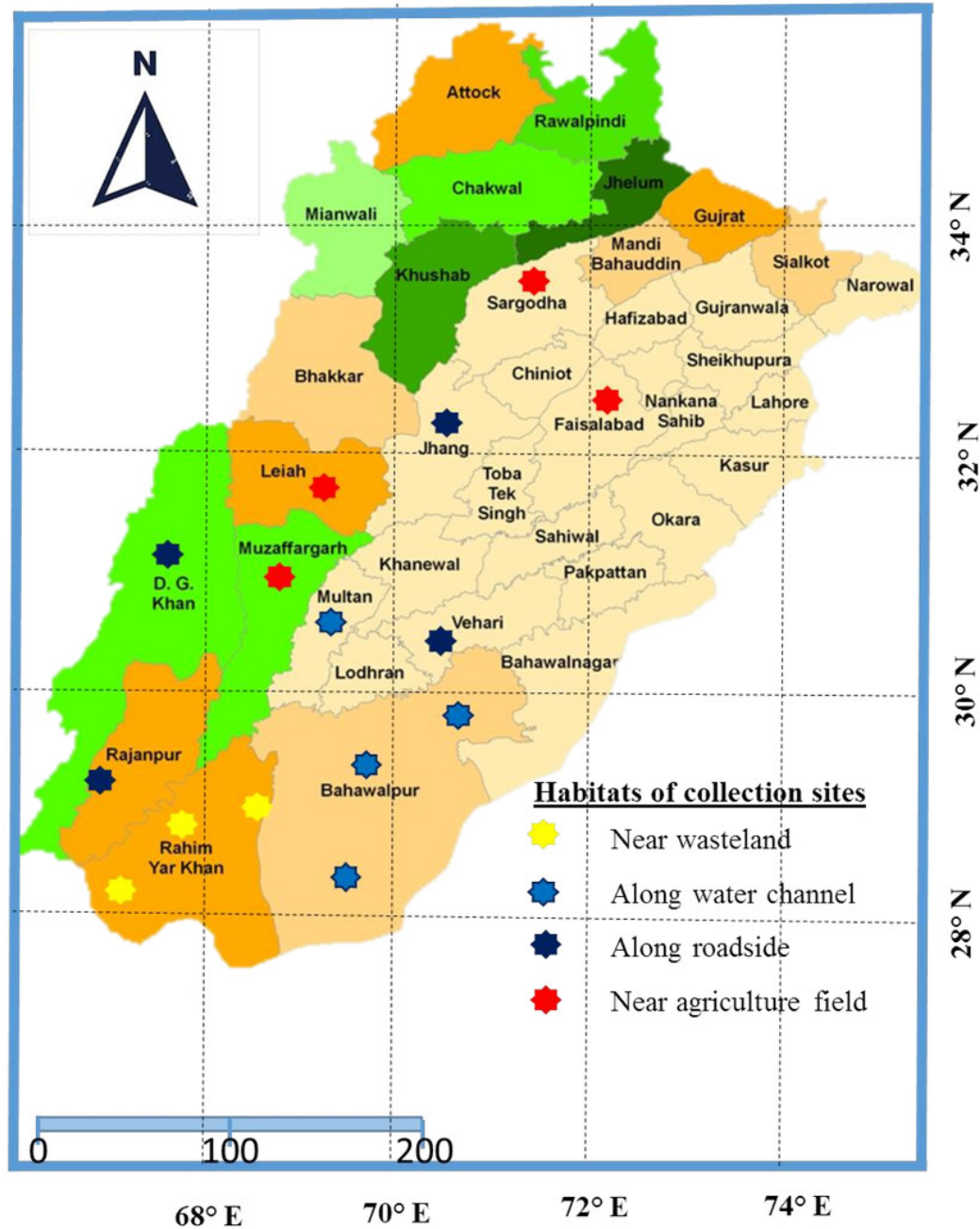


Fig.1. Map of Punjab showing collection sites of *Parthenium hysterophorus* L. sampled from different districts

Figure 2

Habitat view of *Parthenium hysterophorus* L. populations collected from different ecological regions



Fig.2. Habitat view of *Parthenium hysterophorus* L. populations collected from different ecological regions.

Figure 3

Root transvers sections of *Parthenium hysterophorus* L. populations collected from different ecological regions

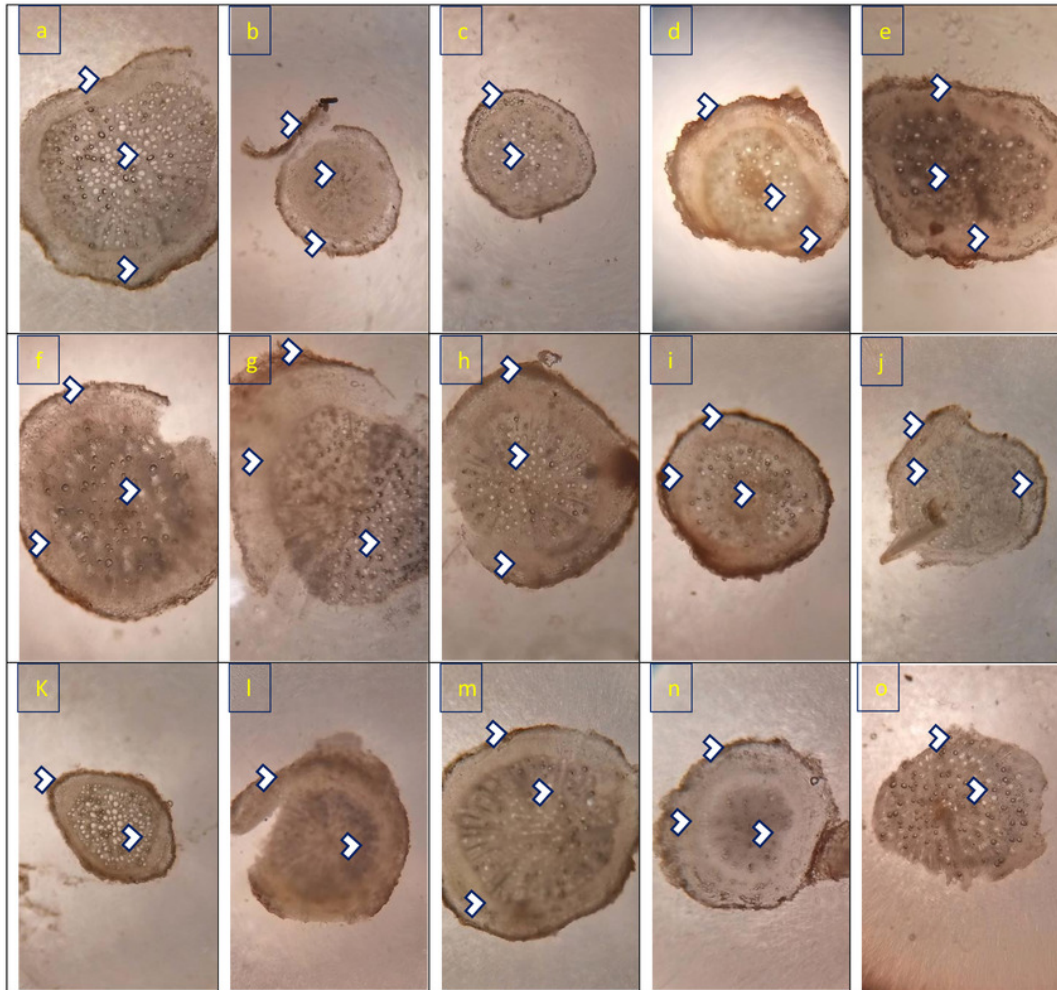


Fig.3. Root transvers sections of *Parthenium hysterophorus L.* populations collected from different ecological regions.

Description: **a. RYK-Rahim Yar Khan.** Thicker epidermis, enlarge cortical region and metaxylem vessels, **b. SDK-Sadiqabad.** Reduced root cellular area, cortical thickness, metaxylem vessels and slightly crushed, **c. KHP-Khanpur.** Reduced root area and epidermal thickness, enhanced metaxylem vessels **d. BWP-Bahawalpur.** Greatly enhanced epidermal thickness, cortical thickness and metaxylem area, **e. LAP-Liaquatpur.** Extraordinarily thicker epidermis, cortical region and metaxylem vessels, **f. AHP-Ahmadpur.** Extraordinarily thick cortical region and enlarge metaxylem vessels, **g. MUL-Multan.** Thick epidermis and cortical region, enhanced metaxylem area, **h. VEH-Vehari.** Thicker epidermis, partially crushed cortical region and enlarge xylem vessels, **i. DGK-DG Khan.** Thick epidermis and cortical region, reduced xylem vessels, **J. RJP-Rajanpur.** Greatly reduced root cellular region and cortical thickness and metaxylem area, **k. JHG-Jhang.** Reduced root area, cortical region and metaxylem vessels, **l. MUZ-Muzaffargarh.** Reduced cortical thickness and partially crushed cortical region, **m. SAR-Sargodha.** Thick epidermis, enlarge metaxylem vessels and cortical region, **n. FSD-Faisalabad.** Thick cortical region and reduced xylem vessels, **o. LYH-Layyah.** Reduced cortical region and metaxylem area.

Figure 4

Stem transvers sections of *Parthenium hysterophorus* L. populations collected from different ecological regions

Description: **a. RYK-Rahim Yar Khan.** Thicker epidermis, enlarge cortical region and vascular bundles, **b. SDK-Sadiqabad.** Reduced stem cellular area, cortex thickness, metaxylem vessels and vascular bundle area, **c. KHP-khanpur.** Enlarge stem area, enhanced cortical and epidermal thickness, sparse hairiness on surface **d. BWP-Bahawalpur.** Greatly enhanced epidermal thickness, cortical and pith thickness, and vascular bundle area, **e. LAP-Liaqatpur.** Extraordinarily thick cortical region, vascular and pith region, thick surface pubescence, **f. AHP-Ahmadpur.** Extraordinary, reduced stem area, pith region and enlarge surface hairs, **g. MUL-Multan.** Thick cortical region reduced vascular bundles and enhanced pith area, **h. VEH-Vehari.** Thicker epidermis, partially crushed cortical region and reduced pith and vascular region, **i. DGK-DG Khan.** Thicker cortical region enhanced vascular bundles and pith region, **j. RJP-Rajanpur.** Greatly reduced stem area, pith thickness and vascular bundle area, **k. JHG-Jhang.** Reduced stem area, vascular region and pith region, **l. MUZ-Muzaffargarh.** Enhanced cortical thickness, vascular region and pith area, **m. SAR-Sargodha.** Thicker epidermis, enlarge vascular bundles and pith region, **n. FSD-Faisalabad.** Thick cortical region, surface hairiness, enlarge vascular bundles and xylem vessels, **o. LYH-Layyah.** Reduced stem area, pith thickness and vascular area.

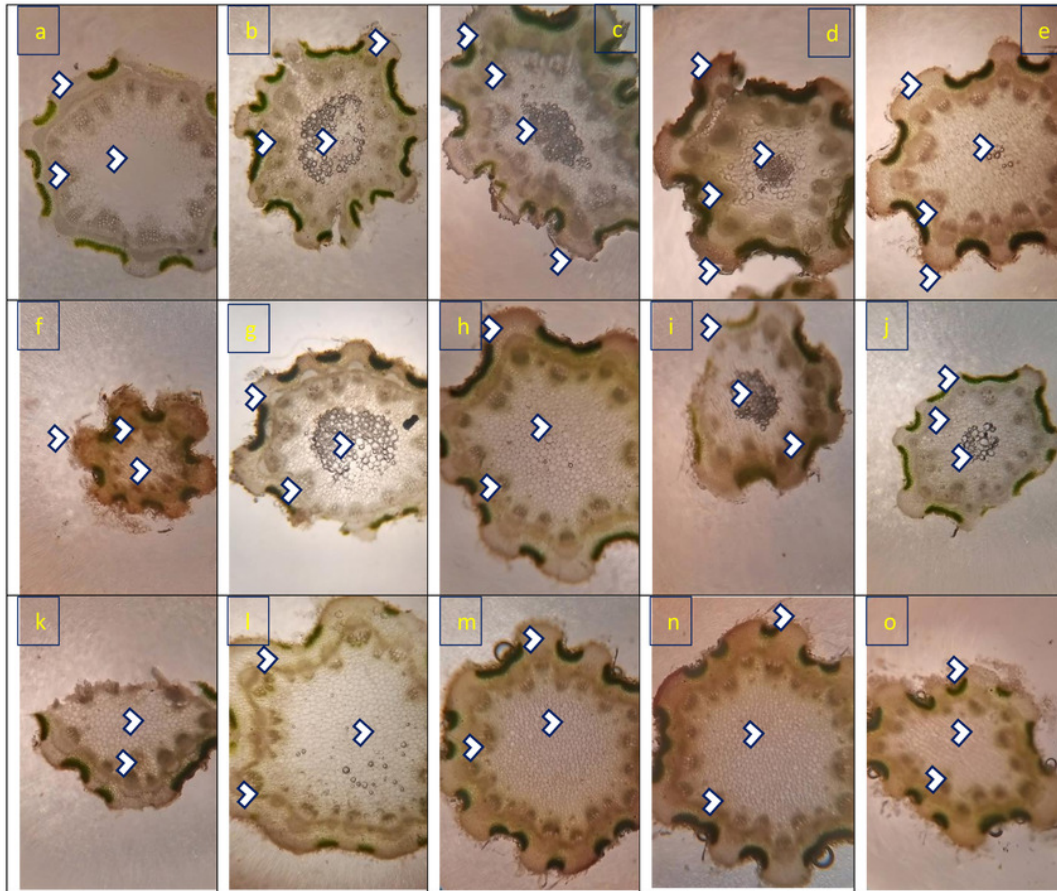


Fig.4. Stem transvers sections of *Parthenium hysterophorus* L. populations collected from different ecological regions.

Description: **a. RYK-Rahim Yar Khan.** Thicker epidermis, enlarge cortical region and vascular bundles, **b. SDK-Sadiqabad.** Reduced stem cellular area, cortex thickness, metaxylem vessels and vascular bundle area, **c. KHP-khanpur.** Enlarge stem area, enhanced cortical and epidermal thickness, sparse hairiness on surface **d. BWP-Bahawalpur.** Greatly enhanced epidermal thickness, cortical and pith thickness, and vascular bundle area, **e. LAP-Liaquatpur.** Extraordinarily thick cortical region, vascular and pith region, thick surface pubescence, **f. AHP-Ahmadpur.** Extraordinary, reduced stem area, pith region and enlarge surface hairs, **g. MUL-Multan.** Thick cortical region reduced vascular bundles and enhanced pith area, **h. VEH-Vehari.** Thicker epidermis, partially crushed cortical region and reduced pith and vascular region, **i. DGK-DG Khan.** Thicker cortical region enhanced vascular bundles and pith region, **J. RJP-Rajanpur.** Greatly reduced stem area, pith thickness and vascular bundle area, **k. JHG-Jhang.** Reduced stem area, vascular region and pith region, **l. MUZ-Muzaffargarh.** Enhanced cortical thickness, vascular region and pith area, **m. SAR-Sargodha.** Thicker epidermis, enlarge vascular bundles and pith region, **n. FSD-Faisalabad.** Thick cortical region, surface hairiness, enlarge vascular bundles and xylem vessels, **o. LYH-Layyah.** Reduced stem area, pith thickness and vascular area.

Figure 5

Leaf transvers sections of *Parthenium hysterophorus* L. populations collected from different ecological regions

Description: **a. RYK-Rahim Yar Khan.** Thicker lamina, enlarge proportion of cortical region and reduced vascular bundles, **b. SDK-Sadiqabad.** Thick leaf in terms of midrib and lamina thickness, enhanced cortex thickness and vascular region, **c. KHP-khanpur.** Reduced leaf thickness, enlarge cortical region and vascular bundle area, **d. BWP-Bahawalpur.** Greatly enhanced epidermal thickness, lamina thickness, cortical thickness and vascular area, **e. LAP-Liaquatpur.** Extraordinarily thick leaf, cortical region and vascular bundles, **f. AHP-Ahmadpur.** Extraordinarily thick cortical region, surface hairiness and reduced vascular bundles, **g. MUL-Multan.** Reduced lamina thickness and epidermal thickness enhanced cortical region and vascular area, **h. VEH-Vehari.** Thicker leaf, epidermis, enhanced cortical region and vascular bundle area, **i. DGK-DG Khan.** Sparse surface hairiness, Thick cortical region, enhanced vascular region, **j. RJP-Rajanpur.** Greatly reduced leaf thickness, cortical thickness and enlarged vascular bundle area, **k. JHG-Jhang.** Thick leaf area, vascular bundles and cortical region, **l. MUZ-Muzaffargarh.** Reduced lamina, cortical thickness and large vascular bundles, **m. SAR-Sargodha.** Thick epidermis, enlarge vascular bundles and cortical region, **n. FSD-Faisalabad.** Reduced leaf area, thick cortical region and reduced vascular bundles, **o. LYH-Layyah.** Enhanced surface hairiness, thickness of cortical region and vascular bundles.

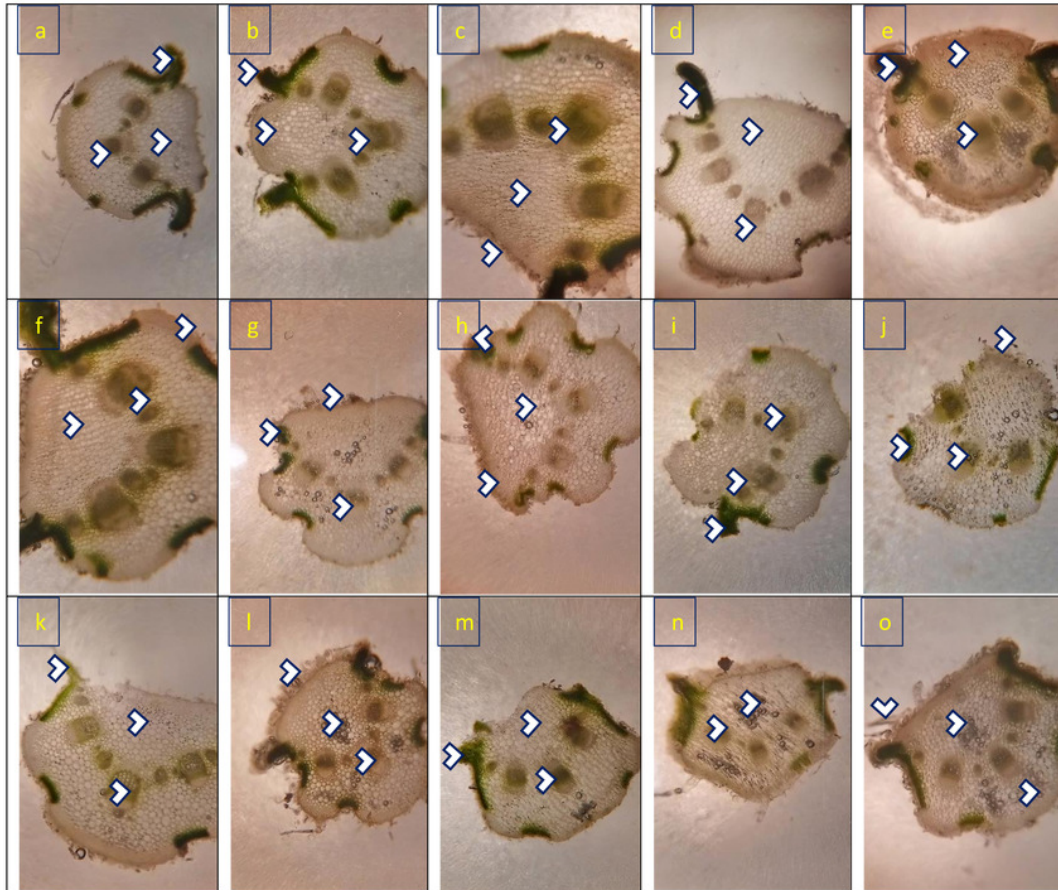


Fig.5. Leaf transvers sections of *Parthenium hysterophorus* L. populations collected from different ecological regions.

Description: **a. RYK-Rahim Yar Khan.** Thicker lamina, enlarge proportion of cortical region and reduced vascular bundles, **b. SDK-Sadiqabad.** Thick leaf in terms of midrib and lamina thickness, enhanced cortex thickness and vascular region, **c. KHP-khanpur.** Reduced leaf thickness, enlarge cortical region and vascular bundle area, **d. BWP-Bahawalpur.** Greatly enhanced epidermal thickness, lamina thickness, cortical thickness and vascular area, **e. LAP-Liaqatpur.** Extraordinarily thick leaf, cortical region and vascular bundles, **f. AHP-Ahmadpur.** Extraordinarily thick cortical region, surface hairiness and reduced vascular bundles, **g. MUL-Multan.** Reduced lamina thickness and epidermal thickness enhanced cortical region and vascular area, **h. VEH-Vehari.** Thicker leaf, epidermis, enhanced cortical region and vascular bundle area, **i. DGK-DG Khan.** Sparse surface hairiness, Thick cortical region, enhanced vascular region, **J. RJP-Rajanpur.** Greatly reduced leaf thickness, cortical thickness and enlarged vascular bundle area, **k. JHG-Jhang.** Thick leaf area, vascular bundles and cortical region, **l. MUZ-Muzaffargarh.** Reduced lamina, cortical thickness and large vascular bundles, **m. SAR-Sargodha.** Thick epidermis, enlarge vascular bundles and cortical region, **n. FSD-Faisalabad.** Reduced leaf area, thick cortical region and reduced vascular bundles, **o. LYH-Layyah.** Enhanced surface hairiness, thickness of cortical region and vascular bundles.

Figure 6

Principal component analysis (PCA) showing influence of soil physicochemical characteristics on A) growth and physiological features, B) root anatomy, C) stem anatomy, D) leaf anatomy of *Parthenium hysterophorus* collected from Punjab province

Figure legends: Collection Sites: RYK-Rahim Yar Khan, SDK-Sadiq abad, KHP-Khanpur BWP-Bahawalpur, LAP-Liaquatpur, AHP-Ahmadpur, MUL-Multan, VEH-Vehari, MUZ-Muzaffargarh, SAR-Sargodha, FSD-Faisalabad, DGK-Dera Ghazi Khan, RJP-Rajanpur, JHG-Jhang, RYK-Rahim Yar Khan. **Soil:** ECe-electrical conductivity, pH-soil pH, OM-organic matter, SP-saturation percentage, PO₄-phosphate, NO₃-nitrate, Cl-chloride, Ca-calcium, Na-sodium, K-potassium. **Physiology:** TSP-total soluble proteins, GB-glycine betaine, Chl a-chlorophyll a, Chl b-chlorophyll b, TChl-total chlorophyll, Car-carotenoids, Chl a/b-chlorophyll a/b ratio, TChl/Car-total chlorophyll/carotenoid ratio. **Morphology:** PH-plant height, SFW-shoot fresh weight, SDW-shoot dry weight, LN-leaf number, RL-root length, RFW-root fresh weight, RDW-root dry weight, LA-leaf area, SL-shoot length. **Root anatomy:** RA-root area, EpT-epidermal thickness, CT-cortical thickness, CCA-cortical cell area, VBA-vascular bundle area, MA-metaxylem area, PhA-phloem area. **Stem anatomy:** SA-stem area, EpT-epidermal thickness, CT-cortical thickness, CCA-cortical cell area, VBA-vascular bundle area, MA-metaxylem area, PhA-phloem area. **Leaf anatomy:** MrT-midrib thickness, LMT-lamina thickness, EpT-epidermal thickness, CT-cortical thickness, CCA-cortical cell area, VBA-vascular bundle area, MA-metaxylem area, PhA-phloem area.

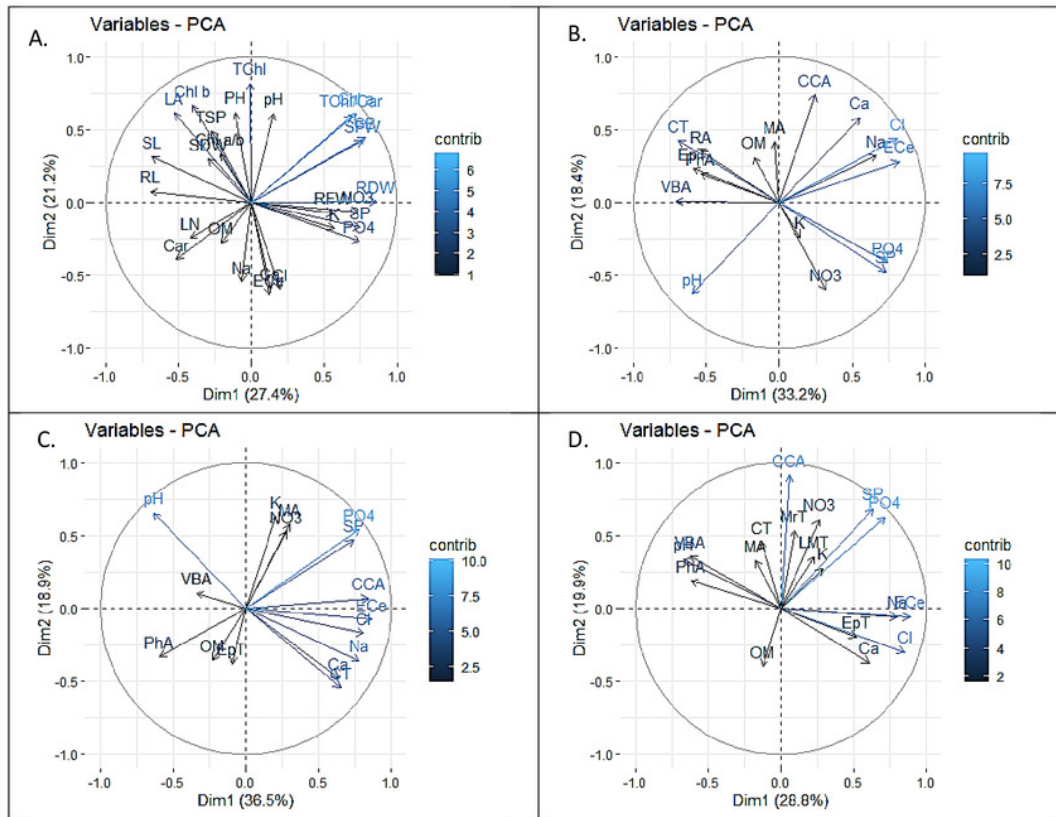


Fig. 6. Principal component analysis (PCA) showing influence of soil physicochemical characteristics on A) growth and physiological features, B) root anatomy, C) stem anatomy, D) leaf anatomy of *Parthenium hysterophorus* collected from Punjab province.

Figure legends: **Collection Sites:** RYK-Rahim Yar Khan, SDK-Sadiq abad, KHP-Khanpur BWP-Bahawalpur, LAP-Liaquatpur, AHP-Ahmadpur, MUL-Multan, VEH-Vehari, MUZ-Muzaffargarh, SAR-Sargodha, FSD-Faisalabad, DGK-Dera Ghazi Khan, RJP-Rajanpur, JHG-Jhang, RYK-Rahim Yar Khan. **Soil:** ECe-electrical conductivity, pH-soil pH, OM-organic matter, SP-saturation percentage, PO4-phosphate, NO3-nitrate, Cl-chloride, Ca-calcium, Na-sodium, K-potassium. **Physiology:** TSP-total soluble proteins, GB-glycine betaine, Chl a-chlorophyll a, Chl b-chlorophyll b, TChl-total chlorophyll, Car-carotenoids, Chl a/b-chlorophyll a/b ratio, TChl/Car-total chlorophyll/carotenoid ratio. **Morphology:** PH-plant height, SFW-shoot fresh weight, SDW-shoot dry weight, LN-leaf number, RL-root length, RFW-root fresh weight, RDW-root dry weight, LA-leaf area, SL-shoot length. **Root anatomy:** RA-root area, EpT-epidermal thickness, CT-cortical thickness, CCA-cortical cell area, VBA-vascular bundle area, MA-metaxylem area, PhA-phloem area. **Stem anatomy:** SA-stem area, EpT-epidermal thickness, CT-cortical thickness, CCA-cortical cell area, VBA-vascular bundle area, MA-metaxylem area, PhA-phloem area. **Leaf anatomy:** MrT-midrib thickness, LMT-lamina thickness, EpT-epidermal thickness, CT-cortical thickness, CCA-cortical cell area, VBA-vascular bundle area, MA-metaxylem area, PhA-phloem area.

Figure 7

Heatmap showing association of soil physiochemical characteristics on A) growth and physiological characteristics, B) root, C) stem and D) leaf anatomical features of *Parthenium hysterophorus* collected from Punjab province

Collection Sites: RYK-Rahim Yar Khan, SDK-Sadiq abad, KHP-Khanpur BWP-Bahawalpur, LAP-Liaquatpur, AHP-Ahmadpur, MUL-Multan, VEH-Vehari, MUZ-Muzaffargarh, SAR-Sargodha, FSD-Faisalabad, DGK-Dera Ghazi Khan, RJP-Rajanpur, JHG-Jhang, RYK-Rahim Yar Khan. **Soil:** ECe-electrical conductivity, pH-soil pH, OM-organic matter, SP-saturation percentage, PO₄-phosphate, NO₃-nitrate, Cl-chloride, Ca-calcium, Na-sodium, K-potassium. **Physiology:** TSP-total soluble proteins, GB-glycine betaine, Chl a-chlorophyll a, Chl b-chlorophyll b, TChl-total chlorophyll, Car-carotenoids, Chl a/b-chlorophyll a/b ratio, TChl/Car-total chlorophyll/carotenoid ratio. **Morphology:** PH-plant height, SFW-shoot fresh weight, SDW-shoot dry weight, LN-leaf number, RL-root length, RFW-root fresh weight, RDW-root dry weight, LA-leaf area, SL-shoot length. **Root anatomy:** RA-root area, EpT-epidermal thickness, CT-cortical thickness, CCA-cortical cell area, VBA-vascular bundle area, MA-metaxylem area, PhA-phloem area. **Stem anatomy:** SA-stem area, EpT-epidermal thickness, CT-cortical thickness, CCA-cortical cell area, VBA-vascular bundle area, MA-metaxylem area, PhA-phloem area. **Leaf anatomy:** MrT-midrib thickness, LMT-lamina thickness, EpT-epidermal thickness, CT-cortical thickness, CCA-cortical cell area, VBA-vascular bundle area, MA-metaxylem area, PhA-phloem area.

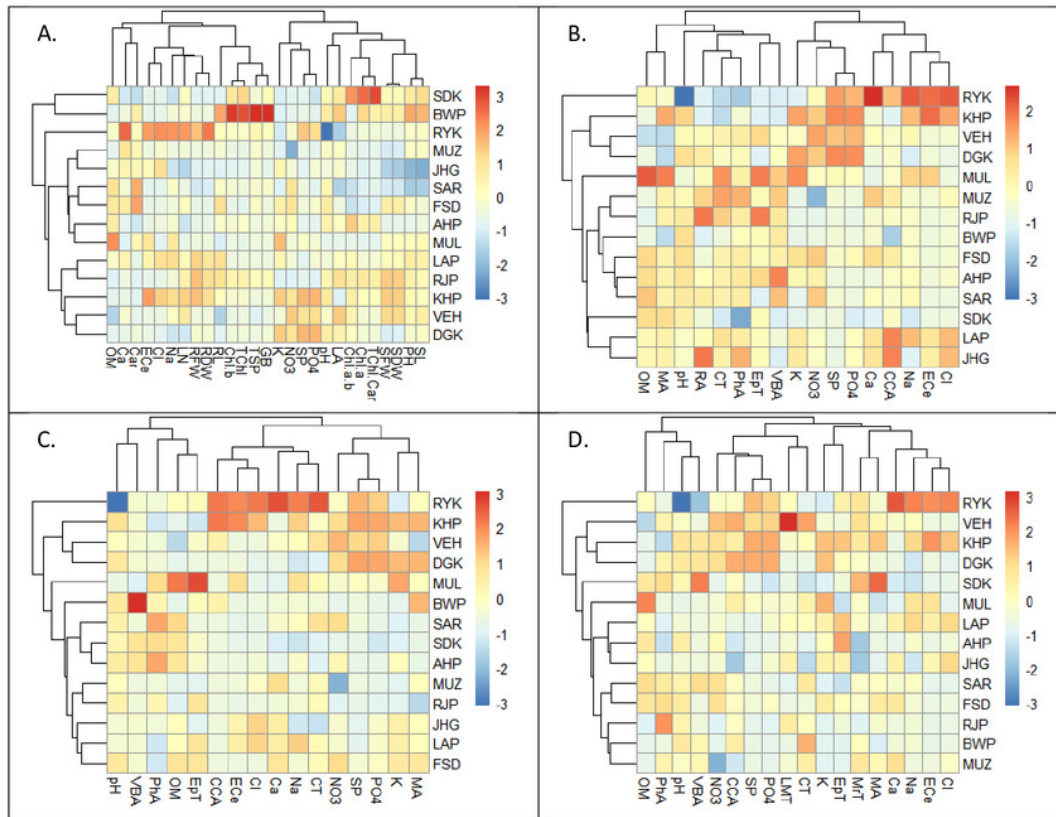


Fig. 7. Preaty heatmap showing association of soil physiochemical characteristics on A) growth and physiological characteristics, B) root, C) stem and D) leaf anatomical features of *Parthenium hysterophorus* collected from Punjab province.

Figure legends: Collection Sites: RYK-Rahim Yar Khan, SDK-Sadiq abad, KHP-Khanpur BWP-Bahawalpur, LAP-Liaquatpur, AHP-Ahmadpur, MUL-Multan, VEH-Vehari, MUZ-Muzaffargarh, SAR-Sargodha, FSD-Faisalabad, DGK-Dera Ghazi Khan, RJP-Rajanpur, JHG-Jhang, RYK-Rahim Yar Khan. **Soil:** ECe-electrical conductivity, pH-soil pH, OM-organic matter, SP-saturation percentage, PO4-phosphate, NO3-nitrate, Cl-chloride, Ca-calcium, Na-sodium, K-potassium. **Physiology:** TSP-total soluble proteins, GB-glycine betaine, Chl a-chlorophyll a, Chl b-chlorophyll b, TChl-total chlorophyll, Car-carotenoids, Chl a/b-chlorophyll a/b ratio, TChl/Car-total chlorophyll/carotenoid ratio. **Morphology:** PH-plant height, SFW-shoot fresh weight, SDW-shoot dry weight, LN-leaf number, RL-root length, RFW-root fresh weight, RDW-root dry weight, LA-leaf area, SL-shoot length. **Root anatomy:** RA-root area, EpT-epidermal thickness, CT-cortical thickness, CCA-cortical cell area, VBA-vascular bundle area, MA-metaxylem area, PhA-phloem area. **Stem anatomy:** SA-stem area, EpT-epidermal thickness, CT-cortical thickness, CCA-cortical cell area, VBA-vascular bundle area, MA-metaxylem area, PhA-phloem area. **Leaf anatomy:** MrT-midrib thickness, LMT-lamina thickness, EpT-epidermal thickness, CT-cortical thickness, CCA-cortical cell area, VBA-vascular bundle area, MA-metaxylem area, PhA-phloem area.